

Astrophysics of Galaxies

Contents

1 Luminosity Function	3
1.1 Measuring the LF	3
1.1.1 Schechter function	4
1.2 Deriving absolute magnitudes	4
1.3 The LF from the Sloan Digital Sky Survey (SDSS)	6
1.4 Galaxy classification	8
1.4.1 Spectroscopic classification	8
1.4.2 Photometric classification	8
1.4.3 Photometric redshift	9
2 Ionized Gas and Stellar Kinematics	10
2.1 Main spectroscopic techniques	10
2.2 Ionized gas kinematics	10
2.2.1 Redshift and velocity measurements	11
2.2.2 Determination of the system velocity and galactic center	11
2.2.3 Deprojection and transformation to physical quantities	12
2.2.4 Instrumental and observational effects that influence kinematic measurements	12
2.3 Stellar component kinematics	13
2.3.1 Effects of the redshift on the spectrum	13
2.3.2 Definition of LOSVD	13
2.3.3 Spectrum of a galaxy as a convolution	14
2.3.4 Deriving the LOSVD	14
2.3.5 Fourier quotient method	14
2.3.6 Higher order moments: h_3 and h_4	15
3 The Local Universe	16
3.1 The Local Group	16
3.2 Clusters of Galaxies	16
3.3 The Virgo Cluster	16
4 Super Massive Black Holes in Galaxies	17
4.1 Theoretical aspects	17
4.1.1 Schwarzschild radius	17
4.1.2 Radius of influence	18
4.2 Super Massive Black Holes	18
4.2.1 Measuring the SMBH mass	18
4.3 Scaling relations for SMBH	19
5 Scaling relations in elliptical galaxies	20
5.1 Formation of elliptical galaxies	20
5.2 Kormendy relation (I_e vs R_e)	20
5.3 Faber-Jackson (L vs σ_0)	21
5.4 The Fundamental Plane	21
5.5 The k -plane	22
5.6 Evolution of the FP with z	22
5.7 The $D_n - \sigma$ relation	23

6 Scaling relations in spiral galaxies	24
6.1 Formation and evolution of spiral galaxies	24
6.2 The Tully-Fisher relation	24
6.3 Tully-Fisher evolution with z	25
6.4 Freeman Law	26
6.5 Low Surface Brightness galaxies	26
7 Interstellar Medium	27
7.1 ISM components	27
7.2 Radio continuum and IR luminosity	28
7.3 ISM in disk galaxies	28
7.3.1 Radial distribution	28
7.3.2 Azimuthal distribution	29
7.3.3 Metallicity	29
7.3.4 Star formation	30
7.4 S0 galaxies	30
7.5 ISM in elliptical galaxies	31
7.5.1 Cold gas in elliptical galaxies	31
8 Dark Matter	32
8.1 Cosmological scenario and dark matter	32
8.2 Dark matter in spiral galaxies	33
8.2.1 Mass distribution models	33
8.2.2 Where does the halo end?	34
8.3 Dark matter in elliptical galaxies	34
8.4 Dark matter in LSB galaxies	34
8.5 Dwarf galaxies	35
8.6 Dark matter and lensing	35
8.7 Alternatives to dark matter: MOND	36

Chapter 1

Luminosity Function

When studying galaxies we can obtain information on their formation and evolution by analyzing their distribution in brightness. This distribution is defined using the **Luminosity Function (LF)** which may be built by measuring the magnitudes in different photometric bands due to the difficulty of measuring the bolometric luminosity. There are several reasons for measuring the luminosity function:

- is an useful tool for comparing the real universe with the one obtained through cosmological simulations;
- gives information about the evolution of galaxies when compared to the redshift;
- the dependence on the environment gives indication about the effects of the environment on the formation and evolution of the galaxies.

The LF depends on the photometric band used (which depends on the kind of information we are aiming at) and galactic structure such as size, central surface brightness, morphological type...

1.1 Measuring the LF

The mathematical function used to describe the LF is denoted by $\Phi(M)dM$, which is proportional to the number of galaxies that have absolute magnitude in the range $(M, M + dM)$. Normally the LF is normalized by imposing:

$$\int_{-\infty}^{\infty} \Phi(M)dM = \nu \quad (1.1)$$

Where ν is the total number of galaxies per unit of volume. In this way $\Phi(M)dM$ indicates the numerical density of galaxies in the magnitude range $(M, M + dM)$. The classical procedure to determine the LF consists in measuring the **apparent brightness**, convert it to **absolute magnitudes** once determined the distance of the galaxies, apply the **K correction** if the redshift is high in order to convert the measured magnitudes into the ones we would have measured at rest. Finally we divide the number of galaxies in each single brightness bin for the volume of the space.

This method is very simple but shows a lot of disadvantages. First we have to correct for the Malmquist-bias, which relates to the fact that we can see brighter objects further away. Then we have to take into account that estimating the distance of galaxies using the Hubble-Lemaître law is an approximate method and we can't avoid these kind of errors (in particular for nearby galaxies for which the peculiar motions can be greater than the recession velocity itself). These effects particularly affects faint galaxies that can be observed only if close so the low luminosity tail of the LF is roughly determined.

A further complication is the assumption that the galaxies in each magnitude interval are evenly distributed in the volume $V(M)$: we know that there are regions in the universe where the density is higher (e.g. Virgo cluster). So for an absolute magnitude M the number of galaxies found in the volume $V(M)$ may depend on how galaxies are distributed in the universe as much as it can depend on $\Phi(M)$. To get a measure of the intrinsic LF is necessary to eliminate the dependency on $V(M)$. The LF varies significantly when looking at field galaxies or cluster galaxies and when we look at different morphological types (we can call this density-morphology relation).

Once these effects are taken into account the LF takes a simple form: the number of galaxies decreases monotonically with increasing luminosity in the low luminosity region, where $\Phi(M)$ decreases almost exponentially with $|M|$. For brightness higher than the characteristic magnitude M^* , $\Phi(M)$ drops dramatically.

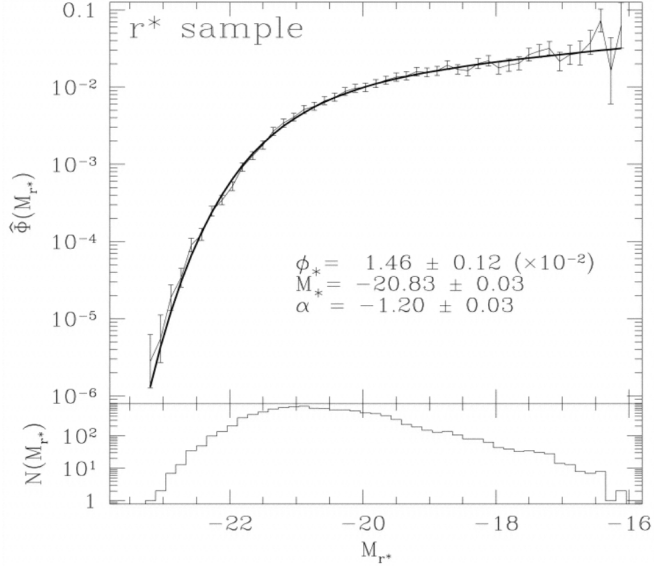


Figure 1.1: Example of a luminosity function, the solid line represent an interpolation with the Schechter function.

1.1.1 Schechter function

A widely used parametrization of the LF is the Schechter function:

$$\Phi(M)dM = (0.4 \ln 10) \phi^* 10^{-0.4(M-M_*)} (\alpha+1) \exp[-10^{-0.4(M-M_*)}] dM \quad (1.2)$$

where ϕ^* , M_* and α are chosen empirically to interpolate the observations. The Eq. 1.2 can be rewritten in terms of luminosity:

$$\Phi(L)dL = \phi^* \left(\frac{L}{L_*}\right)^\alpha \exp\left(-\frac{L}{L_*}\right) dL \quad (1.3)$$

where L_* is the brightness corresponding to the magnitude M_* and indicates the characteristic luminosity after which the number of galaxies falls sharply; ϕ^* determines the normalization of the density of galaxies.

Initially this formula was derived from a model of galaxy formation but they soon realized that it was suitable for many other applications.

1.2 Deriving absolute magnitudes

In determining the LF one of the main things is to derive the absolute magnitude of galaxies. The absolute magnitude M_X in the photometric band X is:

$$M_X = m_X - 5 \log d + 5 - A_X - K_X \quad (1.4)$$

where A_X is the galactic extinction in the X band and K_X is the K correction. We have to determine all these quantities to be able to measure the absolute magnitude of a galaxy.

Extinction due to galactic dust This extinction is due to dust grains present on the galactic plane. The extinction affects more the shorter wavelengths (optical: we can't look at the center of the MW, nIR: the center of the MW is visible) and alters the color of the astronomical sources. This effect is the so-called **color-excess**.

Extinction maps were obtained using the counts of galaxies and the column density of neutral hydrogen as measured by the 21 cm line with radio telescopes. Usually extinction maps coincide with the map of galactic dust. There are regions where the extinction is stronger, like at the galactic poles, and region where this is remarkably low, like in the Lockman hole where there is the minimum HI emission.

The extinction can be determined starting from the color excess and using the table of interstellar extinction. By definition the color excess is:

$$E(B-I) = (B-I) - (B_0-I_0) \quad (1.5)$$

where the second term is the real color. We can estimate the absorption right from the induced change of color (with a little of algebra). Generally the relative extinction in the various bands is known and depends on the properties of the dust and is tabulated in relation to the V band. Once we know the extinction in the V band and the ratio A_X/A_V

(tabulated) we can easily determine the extinction in the X band.

The application of this technique requires the a priori knowledge of the intrinsic color of the observed object, which can be extrapolated through the observation of non-absorbed areas.

K correction By K correction we mean the correction that I have to consider in deriving the apparent magnitude of an object in a given band and considering its redshift. The redshift acts on the observed magnitude in two different ways: first of all the energy is observed in a wider range of wavelengths than it is emitted since the redshift act by translating the spectrum of a constant factor. Therefore a wavelength range emitted $\Delta\lambda$ is seen from the ground as $\Delta\lambda(1 + v/c)$. Since the total flux is not modified by the redshift, the flux per unit of wavelength decreases by a factor $(1 + z)$. In terms of magnitude the attenuation of the spectrum holds:

$$\Delta m = 2.5 \log(1 + z) \quad (1.6)$$

This is not the only effect of the redshift. In fact the observed spectrum is not only **stretched** but also **moved**. It happens that using a given photometric band for measurements the astronomical object is actually observed in a different band.

Since the flux depends on the wavelength of the observation, the apparent magnitude of an object, even taking into account the aforementioned correction, depends on the redshift based on the type of spectrum that characterizes it. In other words, if we are observing in the R band a galaxy with $z = 0.48$, we are actually observing it in the B band. This part of the K correction depends on the morphological type, or on its SED, or on its color. We can conclude that the K correction can be expressed as:

$$K = k(z, \text{morphological type}) + 2.5 \log(1 + z) \quad (1.7)$$

Distance and peculiar motions To compute the absolute magnitude of a galaxy we need to know its distance. Usually it is measured using the **recession velocity** and the **Hubble-Lemaître law** for which:

$$d = V/H_0 \quad (1.8)$$

where we assume $H_0 = 70 \text{ km s}^{-1} \text{ Mpc}^{-1}$. In case of high redshift it is necessary to calculate the luminosity based on more complex expansion models.

There is another component that we have to take into account: the **peculiar motion**. For example if we consider the Virgo cluster we know that it has a recession velocity of about 900 km/s but galaxies are moving inside of it: the average velocity is 1200 km/s and the velocity dispersion σ is of about 600 km/s, so there are both approaching galaxies and receding galaxies with velocities of the order of 2000 km/s.

The fact that a peculiar velocity can be of the order of 500 km/s, means that we can't use the Hubble law in a confident way for galaxies with a redshift lower than 3000 km/s without having huge systematic errors. If in a cluster the recession velocity can be considered the same for all the components so the peculiar velocity is the difference between the observed velocity and that of the cluster.

We can correct for the peculiar velocity of our Galaxy. We know that the Sun moves around the center of the MW with a velocity of about 230 km/s and that our galaxy is moving toward the Virgo cluster at 250 km/s and together they are moving toward the great attractor with a velocity of the order of 600 km/s. All these velocities are known with relatively large uncertainties. Using the CMB dipole anisotropy we can know the exact composition of all these motions and we see that the sun moves at 371 km/s with respect to the cosmic background (high precision measurement). If the object is located in the direction we are moving we have to add 371 km/s to the measured velocity, if the object is exactly at 90° from the apex the correction will be zero. Normally we use the galactic coordinates l (longitude) and b (latitude) in order to calculate the correction using the formula:

$$\Delta V_{3KB} = V_{apex}[\sin(b) \sin(b_{apex}) + \cos(b) \cos(b_{apex}) \cos(l - l_{apex})] \quad (1.9)$$

Total apparent magnitude: the Petrosian radius The measure of the total magnitude of an extended object like a galaxy is not so simple since there is not a net boundary that delimits the edge of a galaxy. It is not advisable to consider too large areas since beyond a certain distance from the center the surface brightness of the galaxies is well below that of the night sky (which varies depending on the band, the moon phase the zodiacal light and the light pollution).

A possibility to overcome this problem is to consider the radius of the isophote to a specific surface brightness. For example in the RC3 catalog is considered as reference isophote the isophote at the surface brightness of 25 mag arcsec $^{-2}$ in B band.

This approach is easy but has some drawbacks: for example if we are in a region with high galactic absorption we underestimate the magnitude of the object since the 25th magnitude isophote will be smaller than that of the galaxy if observed in absence of absorption. Using a reference isophote at a fixed brightness can generate systematic errors.

Last but not least the surface brightness depends on the distance if it becomes sufficiently high: the surface brightness depends on the redshift as $\mu \propto 1/(z+1)^4$.

A method of defining the magnitude is not affected by all these systematic errors makes use of the Petrosian radius defined as:

$$R_p(r) = \frac{\int_{\alpha_{lo}r}^{\alpha_{hi}r} dr' 2\pi r' I(r') / [\pi(\alpha_{hi}^2 - \alpha_{lo}^2)r^2]}{\int_0^r dr' 2\pi r' I(r') / (\pi r^2)} \quad (1.10)$$

The numerator is the average surface brightness at radius r , α_{hi} and α_{lo} are two parameters usually set as 0.8 and 1.25 and define the area within which we have to measure the surface brightness around the radius r . The denominator is instead the average surface brightness within the radius r . This radius is 1 for $r = 0$ and tends to zero for $r \rightarrow \infty$. Usually it is considered the Petrosian radius the radius at which the ratio of Eq. 1.10 is equal to 0.2, as shown in Fig. 1.2 for which the Petrosian radius is $18''$.

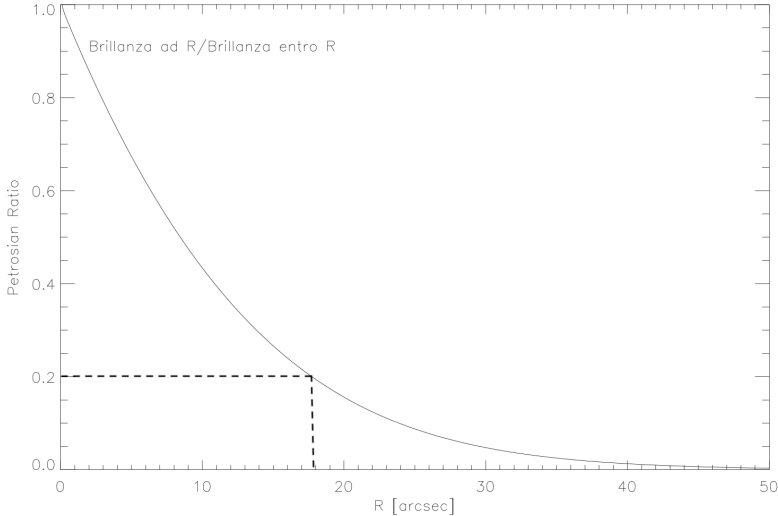


Figure 1.2: Trend of the Petrosian radius described in Eq. 1.10 with the typical value of 0.2.

The **Petrosian magnitude** is the magnitude integrated **within 2 Petrosian radii**. In our example we can see that only 0.6% of the light in the galaxy is emitted outside our $2R_p$ limit of $36''$.

In case of typical seeing the amount of light lost depends on the size of the galaxy and the shape of the profile brightness, in absence of seeing the measured flux is a fixed fraction of that emitted one. However seeing induces a dependence: when the size of the galaxy is similar to that of the seeing, in the case of an exponential disk, about 95% of the light is measured (maximum decrease 0.1 mag).

The Petrosian radius finds important applications in galaxy surveys where algorithms derive the photometric properties in a completely automatic way for thousands of galaxies.

1.3 The LF from the Sloan Digital Sky Survey (SDSS)

SDSS obtained photometric images in 5 bands indicated with the letters u , g , r , i and z . For all galaxies in the sample the redshift was measured spectroscopically and is between 0.016 and 0.2. For the calculation of the absolute magnitude is necessary to measure the distance and the K correction which depends on the morphological type and is derived directly using the color $g-r$. We can use this survey to see the **dependencies** of the Luminosity Function.

Dependence on the redshift The LF can be used to see how galaxies evolve as a population. With the SDSS is possible to measure the LF in a reliable way only for galaxies in the nearby universe ($z < 0.2$), to notice an evolution we have to go further in time, at least at $z = 4$: to do this we need surveys that cover a small solid angle but very deeply, like the FORS Deep Field. The FDF took images in 9 photometric bands that allows to obtain accurate redshift measurements.

We can use this data to determine the LF for each interval of z in the UV band at rest. To avoid too consistent correction we can use observations in photometric bands as much as possible close to the UV band at rest.

If we derive the parameters of the LF from these results the data are comparable with $\alpha = -1.15$ for each z but both ϕ^* and M^* change with continuity showing a clear evolution with z . This observational result can be interpreted as an information on the evolution of galaxies. The UV brightness is linked to the star formation rate according to the

formula:

$$L_{UV} = \text{cost} \cdot \frac{\text{SFR}}{M_\odot \text{ yr}^{-1}} \text{ erg s}^{-1} \text{ Hz}^{-1} \quad (1.11)$$

where by UV we mean the band centered at 280 nm. This shows the evidence that the SFR has changed over time. We can show this dependence using the **Madau plot** (Fig. 1.3): we immediately see that in the past the star formation rate was much higher than in the present epoch, then there is a strong decrease going from $z \sim 2$ to $z = 0$ of approximately one order of magnitude. What happens for $z > 2$ is not clear. The main obstacle to this type of measurements is the absorption due to dust.

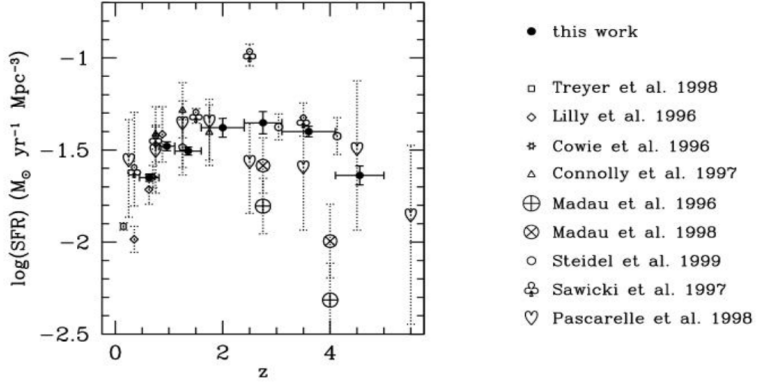


Figure 1.3: Madau plot: cosmic SFR as z varies. The different symbols refer to determinations of SFR made by different authors.

Dependence on the morphological type We already know that elliptical galaxies are in general brighter than spiral galaxies and spiral galaxies of the first types are brighter than late type spiral galaxies. But how can we quantify this?

We need to use an automatic morphological classification method with some mathematical algorithms that analyze the images of the objects. A useful parameter for this purpose is the **concentration index** defined as the ratio between two radii, r_{50} and r_{90} , where r_{50} is the radius which contains half of the light of the galaxy and r_{90} the one that contains 90% of the light:

$$c = \frac{r_{50}}{r_{90}} \quad (1.12)$$

This parameter strongly correlates with the morphological type: the more the galaxy is concentrated (high c value), the more likely is that it is an elliptical galaxy, if less concentrated is a spiral galaxy.

We can now plot the LF as function of two parameters: absolute magnitude and c . In Fig. 1.4 (where $1/c$ is plotted) elliptical galaxies occupy the left side and spiral galaxies are on the right side. In this plot is evident how the luminosity of galaxies decreases going to more advanced morphological types.

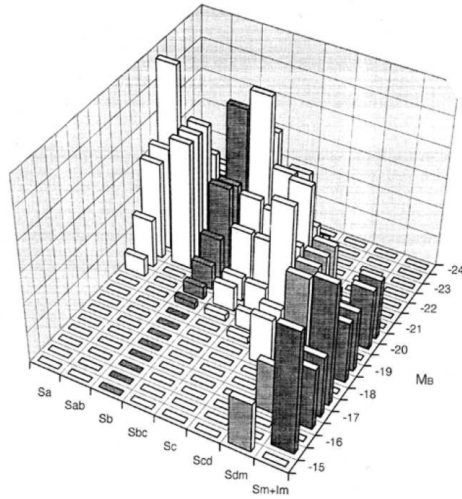


Figure 1.4: LF as function of absolute magnitude and morphological type.

Dependence on the environment The luminosity function depends on the environment. What changes is the fraction of elliptical galaxies and spiral galaxies with the spatial density of galaxies. This effect is called **morphology-density** or **morphology-radius** relation. In less dense environment elliptical galaxies are almost absent while there are spiral and lenticular galaxies with a ratio of about 2:1.

The densest regions of cluster are essentially dominated by elliptical and lenticular galaxies: this phenomenon is explained as an evolutionary effect. According to the hierarchical scenario of evolution of the galaxies, elliptical galaxies are formed by merging of smaller galaxies, which are more likely in region with higher density of galaxies. This mechanism explains the presence of cD galaxies in the center of many clusters.

An alternative way to explain the same effect is in highlighting how the fraction of morphological types changes with the distance from the center of the cluster. But if the morphology-density relation already existed at $z = 0.4$ when the cluster was still evolving, how can it be an evolutionary effect? The main problem is not being able to observe the same cluster of galaxies during its evolution.

1.4 Galaxy classification

1.4.1 Spectroscopic classification

Galaxies can be classified according to their spectrum determined by the stellar population and the ISM. For example an elliptical galaxy is generally poor in dust and HII regions are absent while spiral galaxies are characterized by a younger stellar population and contains HII regions and therefore has emission lines. All this allows to relate the morphological type to the spectrum.

E-type galaxies have a redder spectrum, a marked Balmer jump and only absorption lines, S-type have a blue spectrum with strong emission lines.

Principal Component Analysis PCA is a powerful statistical method that allows to empirically examine correlations between multiple parameters. It consists in calculating the correlation matrix and diagonalizing it by calculating eigenvalues and eigenvectors. In this way a basis of N vectors is identified which best describes the population. Furthermore it allows to identify which are the most characteristic eigenvectors for the population. This allows to reduce the number of parameters necessary to describe an element of the population losing the minimum information.

Galaxy surveys produce a large amount of spectra that allow to measure a large amount of galaxy properties. The spectrum of a galaxy is the measure of its stellar population, its gas content and its dynamic properties. Spectral properties often correlate with the morphology of galaxies. A spectrum can be considered as 1 point in a M-dimensional space where M is the number of bins at which the flow is measured. At this point the spectrum will have M flux measurements, one for each wavelength interval (bin). The aim of the PCA is to find the linear combination of the M parameters along which the variance is the greatest. This is then the principal component that can characterize the input in the most efficient way. It is possible to see that this axis corresponds to the eigenvector corresponding to the greatest eigenvalue.

Giving a physical sense to the PCAs we have:

- **PC1**: shows the correlation between the slope of the continuum in the blue and the presence of strong emissions;
- **PC2**: allows to increase the intensity of the emissions without altering the shape of the continuum;
- **PC3**: allows an anti-correlation between the intensity of the oxygen and $H\alpha$ lines, in relation to the ionization level of the regions that generate the emission.

We can consider two approaches to give a physical meaning to the PCA analysis on the spectra of galaxies: we can interpret the spectrum or proceed with a morphological classification.

1.4.2 Photometric classification

Galaxies can be classified using three model-independent parameters measured on a single galaxy image that can reveal its major ongoing and past formation modes. These parameters quantitatively measure: the concentration (C), the asymmetry (A) and the clumpiness (S) of a galaxy's stellar light distribution. When combined into a three dimensional CAS volume, all major classes of galaxy in various phases of evolution are cleanly distinguished.

Concentration (C) Elliptical galaxies are concentrated systems while spiral galaxies are less concentrated because of their rotation. The concentration of light can therefore be used to distinguish between the two classes:

$$C = 5 \log \left(\frac{r_{out}}{r_{in}} \right) \quad (1.13)$$

There are several ways to choose r_{in} and r_{out} , for distant galaxies it is convenient using the Petrosian radius. A definition that is often used is $r_{in} = r_{20\%}$ and $r_{out} = r_{80\%}$.

Elliptical galaxies have $C > 4$ while spiral galaxies have $4 > C > 3$.

Asymmetry (A) The asymmetry index quantifies the phenomena that generate asymmetries, like star formation, interactions, merging and dust bands. It is expressed as:

$$A = \frac{\text{abs}(I - R)}{I} \quad (1.14)$$

where I is the initial image and R is the image rotated by 180° . Images are typically smoothed with a filter of size $1/6r_{Petr}$: this means that the image is convolved with a Gaussian filter with a fixed radius that eliminates all the fluctuations or structures smaller than the filter size. A structureless galaxy (elliptical) will have a small A value while one with structures (spiral arms, HII regions) will have a large A .

High-Spatial Frequency Clumpiness (S) There are several ways a galaxy can contain clumpy material at high spatial frequencies. For example while most ellipticals are smooth and therefore contain only low-frequency, galaxies with ongoing star formation are very patchy and contain large amounts of light at high frequencies. To quantify this we can use the clumpiness index defined as the amount of light contained in high frequency structures to the total amount of light in the galaxy. For ellipticals this ratio should be near zero.

The image of the galaxy is first convolved with a Gaussian filter to eliminate all fluctuations or structures smaller than the filter size, then the clumpiness index is computed as:

$$S = \frac{I - B}{I} \quad (1.15)$$

where I is the original image of the galaxy and B is the image after being smoothed (blurred).

1.4.3 Photometric redshift

There is a technique that allows to derive the redshift of an object on the basis of photometric measurements in multiple photometric bands. The images must be flux calibrated and, once combined together, they provide a sort of very low resolution spectrum. This spectrum is then compared with a spectra library with different redshift and different spectral types.

This technique must be well calibrated using galaxies that are also observed spectroscopically to determine the degree of uncertainty.

Chapter 2

Ionized Gas and Stellar Kinematics

The study of the kinematics of a galaxy is based on the spectroscopic analysis of its light. The main purpose to study the kinematics is to analyze the mass distribution of the galaxy.

The kinematic is determined by the sum of the contributions from all the components, bright and dark that contribute to its mass. Knowing the stellar kinematics allows us to determine the distribution function, which describes the position and the velocities of the stars. Different scenarios of formation provide a different form of the distribution function.

2.1 Main spectroscopic techniques

Long-slit spectroscopy (mono-dimensional) Is the observation technique most used in the past for galactic kinematics. A traditional spectrograph is in fact made up of a slit, a collimator, a dispersing elements and a CCD camera. This configuration allows to get kinematic information along an axis of the galaxy. The spectrograph is generally oriented to have a slit aligned with the major axis of the target galaxy. This kind of spectrography requires to have a large detector (long to have a good spectral range and wide to allow a long slit).

Integral Field Units (bi-dimensional) This instrument allows to measure spectra on a two dimensional field. The first class of such instruments is the one that uses the Fabbry-Perrot technique: the observation consists in taking a series of images of the galaxy by changing the filter wavelength image after image. For example if we want to measure the H α kinematics ($\lambda 6562.8 \text{ \AA}$) we may set a bunch of filters going from 6551 \AA to 6570 \AA . The major obstacles are:

- limited wavelength obtainable in a reasonable total integration time on the object (each pose must last several minutes);
- difficulty of combining the images obtained at different wavelengths due to conditions of the sky, seeing etc.

One of the main advantages is the large field of view that can be several arcminutes.

A more modern class of instruments is that of **integral field units** (IFU) in which the field is divided into a rectangular matrix or square points, then for each point is obtained a spectrum with a normal spectroscope. In the first case we have optical fibers and we obtain several classic spectra, in the second one we have a slit-less spectrum.

The advantages of IFU are the high sensitivity and the high spatial resolution.

2.2 Ionized gas kinematics

Once we get the spectrum of a point of the galaxy we want to derive the kinematics of the ionized gas. To do so we have to follow these steps:

1. derive the wavelength and the spectrum;
2. transform redshift into velocity;
3. symmetrize the rotation curve by determining the kinematic center and its radial velocity;
4. correct the velocity of the galaxy for the motion of the earth around the sun and for the movement of the sun with respect to the cosmic background;
5. calculate the galaxy's distance and its scale;
6. deproject the observed quantities and transform them into physical units.

2.2.1 Redshift and velocity measurements

The emission lines of the ionized gas are characterized by a low velocity dispersion due to the dissipative nature of the gas that moves it in circular orbits. The asymmetric drift formula shows that where the average velocity of a tracer coincides with the circular velocity, the velocity dispersion is zero (narrow emission line).

To characterize an emission line we interpolate the line with a Gaussian function, determining its average wavelength, its width and intensity. The redshift is defined as:

$$z = \frac{\lambda_{obs} - \lambda_{lab}}{\lambda_{lab}} = \frac{\Delta\lambda}{\lambda} = \frac{\lambda_{obs}}{\lambda_{lab}} - 1 \quad (2.1)$$

The measure of λ is made along the whole slit so to have a measurement in different positions (different distance from the center of the galaxy, initially measured in arcsec, then converted to pc using the scale).

To transform z into velocity we can use the relativistic formulas:

$$V = c \frac{(z+1)^2 - 1}{(z+1)^2 + 1} \quad \text{or} \quad z = \sqrt{\frac{1+V/c}{1-V/c}} - 1 \quad (2.2)$$

For $V \ll c$ we can use the approximation $V = cz$.

2.2.2 Determination of the system velocity and galactic center

Assuming that the rotation curve of a galaxy is symmetric with respect to its kinematical center, it is possible to determine its position finding the center of symmetry of the rotation curve. Doing this we derive the system velocity of the kinematical center.

The velocity derived is the observed radial velocity (V_{radial}) which is the composition of several motions, the main ones are:

- $V_{cosmological}$ velocity of the galaxy due to expansion of the universe
- $V_{p,gal}$ peculiar velocity of the observed galaxy
- $V_{p,Gal}$ peculiar velocity of our galaxy
- V_\odot motion of the Sun around the center of our galaxy
- V_{rev} motion of the Earth around the Sun
- $V_{diurnal}$ rotation of the Earth

Dealing with radial velocity we are only interested in velocity projection along the line of the sight. To derive the distance using the Hubble law we are interested about $V_{cosmological}$. $V_{diurnal}$ is always negligible since is very small. V_{rev} depends on the direction we are looking and the day of the year, and can be worth the maximum 33 km/s so we need to correct.

V_\odot and $V_{p,Gal}$ can be computed together and depend only on the position of the object on the celestial plane. This composition gives the correction ΔV_{3KB} .

There is no way to know $V_{p,gal}$ only knowing the observed radial velocity of a galaxy. If a galaxy is part of a group or a cluster we can use the mean velocity of the group or the cluster. To summarize we have:

$$V_{cosmological} = V_{radial} + \Delta V_{3KB} + V_{rev} \quad (2.3)$$

Once $V_{cosmological}$ is known we can derive the distance of the object using the Hubble law. In case of small speed we can use the approximate formula:

$$D = V_{cosmological}/H_0 \quad \text{where} \quad H_0 = 73 \text{ (km/s)/Mpc} \quad (2.4)$$

With the distance we can derive the spatial scale of the galaxy:

$$\text{scale} = D(\text{pc})/206264.8 = D(\text{Mpc})/0.2062648 \quad (2.5)$$

If we are working with high recession velocities we have to use a more complex formula, distinguishing between angular distance and distance in brightness. To compute these distances we have to use the co-moving distance D_M which depends on the kind of universe we are considering.

2.2.3 Deprojection and transformation to physical quantities

At this point all we have to do is to de-project the observed quantities. We have two particular velocity field: **rigid motion** and **constant velocity**.

Rigid motion The velocity is proportional to the distance from the center like in the case of a rigid body:

$$V(R)_{dep} = \Omega R \quad (2.6)$$

This kind of velocity field is often found in the central region of disk galaxies. In this case we see that, given that in the plane of the sky $x = r \cos \phi$, we can write:

$$V(x, y) = \Omega R \cos \theta \sin i = \Omega r \frac{\cos \phi}{\cos \theta} \cos \theta \sin i = \Omega x \sin i \quad (2.7)$$

Constant velocity Rotation curves in the outer regions of disk galaxies often show a constant value for velocity. A velocity field of this kind appears in projection into the sky:

$$V(R)_{dep} = V_0 \quad (2.8)$$

so in this case we can write:

$$V(r, \phi) = V_0 \cos \theta \sin i = V_0 \frac{\sin i \cos i}{\sqrt{\cos^2 i + \tan^2 \phi}} \quad (2.9)$$

that depends only on ϕ that is the position angle in the sky.

A typical velocity field of a disk galaxy is similar to a rigid motion in the central regions and tends to have $V = \text{constant}$ in the outer region.

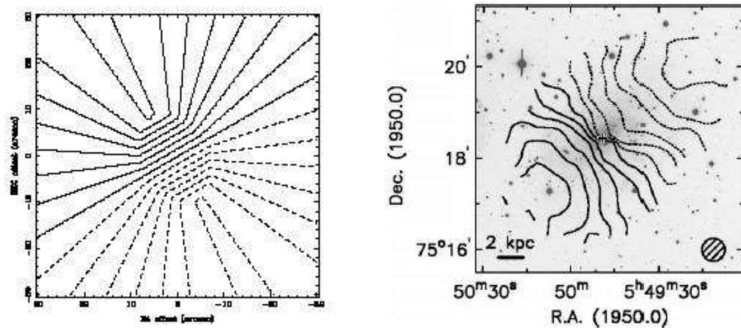


Figure 2.1: Projected velocity of a rigid rotation in the center and a constant velocity in the outer region (left), and the velocity field observed in a real case using HI radio observations (right).

2.2.4 Instrumental and observational effects that influence kinematic measurements

There are two factors that most influence the long-slit kinematical measurements. These are the **atmospheric seeing** and the **slit width**. These are of the order of a few arcsec or a fraction so in the case of nearby galaxies the kinematic measurements is deteriorated in a minimal way and it is not always necessary to take into account those effects. It is instead very important in the case that the features we want to observe vary significantly on angular scales of the order of those indicated.

Point Spread Function convolution The PSF is the image we observe of a point-like source, from the ground is mostly due to atmospheric seeing. For many applications the PSF is assumed to have a two-dimensional shape and is characterized by the value of σ . The expression for a Gaussian PSF is :

$$PSF(x, y) = \exp \left(\frac{-x^2 - y^2}{2\sigma_{seeing}^2} \right) \quad (2.10)$$

The observed image is then the convolution of the light from the galaxy is $I(x, y)$ with the PSF.

In first approximation the PSF actually moves the image with respect to the slit of the spectroscope. The velocity

measured in the position (x, y) will be the convolution of the intrinsic velocity field with the PSF weighted for the intensity at that coordinates.

The function $I(x, y)$ is not known a priori, it is the intrinsic intensity of the galaxy we are observing.

A possible solution is to use images taken from space telescope which are not affected by atmospheric seeing and are characterized by a PSF due exclusively to the instrument.

Slit width larger than the object There are situations where the slit width is larger than the PSF (always true when using STIS telescope on HST). When in this situation we have to take into account the position of the source within the slit. The space information overlaps with the wavelength information.

2.3 Stellar component kinematics

There are galaxies without ionized gas for which is possible to derive dynamical information only from the stellar component. Is the case of **elliptical galaxies** and **S0**. The spectrum of stellar component is characterized by absorption lines. The kinematical measurements is more difficult for the following reasons:

- absorption lines are weaker than emission ones, more precisely the absorption line is always weaker than the continuum;
- there are no isolated absorption lines, they are often in blend with nearby lines so we can't simply use Gaussian interpolation as generally done for the ionized gas;
- the stellar component has a velocity dispersion which can be dynamically more relevant than the velocity itself as in the case of elliptical galaxies, therefore must V and σ must be measured.

2.3.1 Effects of the redshift on the spectrum

Stellar kinematics are measured from the analysis of a spectral region relatively extended in wavelength. The more frequent used region is 4700-5400 Å where we find H β and the MgI lines, Fe and Ca, or the red region 8400-8900 Å around the CaII triplet.

The redshift acts on the spectrum emitted bu the stars moving it towards the red. It is important to note that this shift is not the same for all wavelengths. Being:

$$z = \frac{\Delta\lambda}{\lambda_0} \approx V/c \quad (2.11)$$

it can be easily derived that:

$$\lambda = \lambda_0(1 + V/c) \quad \text{or} \quad \Delta\lambda = \lambda_0V/c \propto \lambda_0 \quad (2.12)$$

However if we use the logarithms the dependence from λ_0 is gone and the spectrum is shifted by a constant quantity so in the logarithmic space redshift acts as a rigid shift. In fact we have:

$$\ln(\lambda) = \ln(\lambda_0) + \ln(1 + V/c) \quad (2.13)$$

and therefore

$$\ln(\lambda) - \ln(\lambda_0) = \Delta(\ln(\lambda)) = \ln(1 + V/c) \approx V/c \quad (2.14)$$

2.3.2 Definition of LOSVD

We introduce the concept of line of sight velocity distribution or more briefly LOSVD(v) that is nothing but the intensity of the emission coming from gas with velocity v or, if we are considering the stellar component, is the function that describes the percentage of stars with radial velocity v . For example a Gaussian LOSVD will have the form:

$$\text{LOSVD}(v; V, \sigma) = \text{NORM} \cdot \exp(-((v - V)/\sqrt{2}\sigma)^2) \quad (2.15)$$

In this case knowing the LOSVD means knowing the two parameters V and σ . The ionized gas typically has a Gaussian LOSVD with σ of a few km/s. Essentially the LOSVD is the unknown factor of our problem. To measure the stellar kinematics means to determine its LOSVD.

2.3.3 Spectrum of a galaxy as a convolution

Because of Eq. 2.14 we see how the spectrum $s^i(\ln \lambda)$ of a generic star i with radial velocity v will be seen from the ground as:

$$s_v^i(\ln \lambda) = \int s^i(\ln \lambda') \delta(\ln \lambda' - \ln \lambda - v/c) d\ln \lambda' \quad (2.16)$$

where δ is a Dirac delta so $s^i(\ln \lambda)$ will always be equal to 0 and different from zero only when $\ln \lambda' - \ln \lambda - v/c = 0$ which means a translation of $s^i(\ln \lambda)$ by an amount equal to v/c .

The spectrum of a point on the galaxy can be seen as the sum of a thousand stars. Strictly speaking the spectrum of a galaxy could then be mathematically described as:

$$G(\ln \lambda) = \sum_i s^i(\ln \lambda') \delta(\ln \lambda' - \ln \lambda - v^i/c) d\ln \lambda' \quad (2.17)$$

where the sum is done on all the stars i .

We can see that the spectrum of an elliptical galaxy is well reproduced by the spectrum of a giant star of type G8-K3 (that now we indicate by $s(\ln \lambda)$). Given that the spectrum $s(\ln \lambda)$ no longer depends on the star i we can change the sum with an integral but the sum of the deltas, each with the velocity of the star is nothing more than the LOSVD. We can rewrite the last equation as:

$$G(\ln \lambda) = \int s(\ln \lambda') LOSVD(\ln \lambda - \ln \lambda') d\ln \lambda' \quad (2.18)$$

In order to find the values of V and σ we compare the spectrum of a galaxy with that of a star convoluted with Gaussian LOSVD with different values of V and σ . We vary these parameters till the spectrum of the galaxy appears to be well reproduced by the convolved stellar spectrum.

2.3.4 Deriving the LOSVD

As we said determining the stellar kinematics means determining the LOSVD. There are several techniques to do so but all of them use the spectrum of one template star and are therefore affected by the so called "template mismatching". This difference is propagated by increasing the uncertainty with which LOSVD is measured. The main determination techniques are:

- **Direct interpolation:** minimize the difference between the observed spectra of the galaxy and that of the star after convolving it with an appropriate value of V and σ (the ones that minimize the mean square difference between the spectrum of the galaxy and the convolved star). Advantages of this method are the fact that there is the possibility of masking the regions of the spectrum disturbed. It is a method very sensitive to template mismatching.
- **Correlation function**
- **Expansion in sum of Gaussian**
- **Fourier quotient**

2.3.5 Fourier quotient method

This method is based on the consideration that the convolution becomes, in the Fourier space, a simple multiplication. We can then write the Eq. 2.18 which is the convolution of $s(\ln \lambda)$ with $LOSVD(\ln \lambda)$ as:

$$\tilde{G} = \tilde{s} \times \tilde{LOSVD} \quad (2.19)$$

where the symbol \sim indicates the Fourier transform. The terms \tilde{G} and \tilde{s} are known from observations. We can then write:

$$LOSVD = \tilde{G}/\tilde{s} \quad (2.20)$$

Once $LOSVD$ is known we can get the LOSVD by applying the Fourier anti-transform. The operation is repeated for the spectra G in the various position of the galaxy in order to obtain the measurement of the kinematics in the whole area (e.g. along the slit) and derive the rotation curve $V(r)$ and the velocity dispersion $\sigma(r)$.

2.3.6 Higher order moments: h_3 and h_4

When the S/N ratio of a spectrum is sufficiently high it is possible to measure even higher order characteristics such as the skewness and the kurtosis. From the mathematical point of view I can characterize the LOSVD based on the value of moments of different orders.

Velocity is the central moment of order 1:

$$V = \frac{\int v \times LOSVD(v)dv}{\int LOSVD(v)dv} \quad (2.21)$$

the **velocity dispersion** is the second order moment with respect to V :

$$\sigma = \sqrt{\frac{\int (v - V)^2 \times LOSVD(v)dv}{\int LOSVD(v)dv}} \quad (2.22)$$

In the same way we can define the higher moments of **skewness** and **kurtosis** as:

$$\text{skewness} = \frac{\int (v - V)^3 \times LOSVD(v)dv}{\int LOSVD(v)dv} \quad (2.23)$$

$$\text{kurtosis} = \frac{\int (v - V)^4 \times LOSVD(v)dv}{\int LOSVD(v)dv} \quad (2.24)$$

In practice skewness and kurtosis are not used to parametrize the shape of the LOSVD but is used in the expansion of Gauss-Hermite. The LOSVD is described according to the form:

$$LOSVD(v) = I_0 \exp(-y^2/2)(1 + h_3 H_3(y) + h_4 H_4(y)) \quad (2.25)$$

where $y = (v - V_0)/\sigma_0$ and H_3 and H_4 are the Hermite polynomial of 3rd and 4th degree.

H_3 describes the asymmetric deviations from the Gaussian form and therefore the coefficient h_3 will be much higher the more the LOSVD is asymmetric. A negative value indicates an asymmetric tail for values smaller than the mean velocity, a positive values for larger values. H_4 describes the symmetric deviations such as flatness or sharpness. The coefficient h_4 is positive if the LOSVD is more cuspy and negative if it is more top flat.

The two parameters are not correlated so an error induced by the noise to this values will not affect the measure of the other parameter.

Usually the stellar LOSVD, unlike the emission lines of gas, has nonzero values of h_3 and h_4 .

Chapter 3

The Local Universe

3.1 The Local Group

The Local Group (LG) is the system in which our galaxy is located. It consists of about 35 galaxies, mostly dwarf ellipticals (dE) and dwarf spheroids (dSph) and some irregular dwarfs (dIrr). It is dominated by two giant spiral galaxies: the Milky Way and the Andromeda Galaxy. Our knowledge of the LG is not complete: there are areas that are not visible behind the MW and dwarf galaxies farther than 500 kpc are difficult to observe. We can estimate a completeness of about 75 %.

In the local group there are only three spiral galaxies: the aforementioned Milky Way and Andromeda (M31) and M33, also called Triangulum galaxy. The luminosity of the Local Group is dominated by the Milky Way and M31.

The Local Group member next in luminosity is the Large Magellanic Cloud followed by the Small Magellanic Cloud. Both are satellite galaxies of the Milky Way and belong to the class of irregular galaxies.

Many of the dwarf galaxies grouped around the MW or around M31. Their spatial distribution shows a peculiarity: they form a highly flattened disk that lie in a plane which is oriented perpendicular to the galactic plane. This is called the **supergalactic plane**. A dwarf galaxy (Sagittarius Dwarf) has been recently identified and it is in the final phase of a merging process with our galaxy. The body of the galaxy is located almost behind the GC but the tidal tail surrounds the MW in an almost polar position.

3.2 Clusters of Galaxies

George Abell in 1958 was the first to systematically study galaxy clusters. The currently most complete catalog is that of Abell, Corwin and Olowin (ACO) which contains 4073 clusters.

ACO has defined the following criterion for defining a cluster as rich: it must have at least 50 members with a magnitude $m < m_3 + 2$ where m_3 indicates the magnitude of the third brightest member.

Abell classified circular symmetry clusters concentrated in the center as regular (like globular clusters): clusters of this type are rich in S0 and elliptical. Coma and Corona Boreale clusters belong to this class.

In 1974 Oemler identified the following classes:

- **cD clusters**: they have a dominant cD galaxy in the center, contain elliptical, lenticular and spiral galaxies according to a 3:4:2 ratio. Therefore only 20% are spiral galaxies.
- **Spiral-rich clusters**: have an E:S0:S ratio of type 1:2:3

The remaining clusters are classified as **spiral-poor clusters**. According to Abell there is a relationship between the structure of a cluster and the content of galaxies: this was quantified by Oemler who established that in cD clusters the density of galaxies increases rapidly towards the center while spiral-rich clusters are irregular and not very concentrated.

3.3 The Virgo Cluster

The Virgo Cluster is composed of about 150 main galaxies of various morphological types and at least 1000 dwarf galaxies. In the center there are 3 giant elliptical galaxies, M84, M86 and M87, that probably formed from the union of many small galaxies. This cluster has a diffuse X-ray emission (hot gas).

Chapter 4

Super Massive Black Holes in Galaxies

4.1 Theoretical aspects

A black hole is defined as a massive object that exercise a gravitational attraction so intense to prevent matter and even light of moving away from it. Its mass can be considered shrunken in a dimensionless point. A BH is characterized by an imaginary surface whose radius is proportional to its mass.

A BH is essentially the result of a space-time distortion due to the presence of a strong gravitational field. The rays of light that pass close to the BH are deflected along a closed circular trajectory near the center of gravity. The surface of a BH, called the **horizon** is a closed surface of separation within which the escape velocity is greater than the velocity of light: no physical event that happens inside the horizon can communicate its existence or effects on the outside.

Black holes are indicated as BH if they are stellar mass black holes, IBH if we are talking about intermediate mass black holes ($10^3 M_\odot$) and as SMBH if over $10^6 M_\odot$. There are various evidences that in the center of the galaxies there are black holes with masses of the order of $10^6 - 10^9$ solar masses. These SMBH are responsible for the activity of quasars and active galaxies. This activity was more present in the past as indicated by the evolution in z of the LF of the quasars (greater brightness at greater redshift).

4.1.1 Schwarzschild radius

The most important parameter of a BH is its mass M_{BH} which determines the size of the object and the intensity of the associated gravitational field. To describe a BH we can use a test particle of mass m , subject to the gravitational field of a mass M , which escapes with an escape velocity such as to have a velocity equal to zero to infinity. The total energy of this particle is:

$$\frac{1}{2}mv^2 - \frac{GM}{R} = 0 \quad (4.1)$$

and the minimum escape velocity is:

$$v^2 = \frac{2GM}{R} \quad (4.2)$$

Since an object can't move faster than light we can consider $v = c$. In this way we write the Schwarzschild relation for the radius R_S of a black hole:

$$R_S = \frac{2GM_{BH}}{c^2} \quad (4.3)$$

The Schwarzschild does not represent a singularity, is just the region from which is no longer possible to leave.

The volume of a BH built on R_S is then:

$$V_S = \frac{4\pi R_S^3}{3} \quad (4.4)$$

so the density for a BH of generic mass M is:

$$\rho_S = \frac{M}{4\pi R_S^3/3} \quad (4.5)$$

therefore:

$$\rho_S = \frac{3c^6}{4\pi G^3 M^2} \quad (4.6)$$

For a SMBH of mass $10^9 M_\odot$ the density necessary to form it is 150 kg/m^3 or less than the density of water. On the other hand for a BH of $1 M_\odot$ the density reaches a very high value, equal to $1.5 \cdot 10^{20} \text{ kg/m}^3$.

4.1.2 Radius of influence

The term radius of influence indicates the distance from the SMBH beyond which the mass dominating the motion of the tracers is not that of the SMBH but that of the galaxy itself. In order to measure the mass of the SMBH is therefore necessary to have kinematic information within the radius of influence. We can express the circular velocity due to the mass of the galaxy as $M(r) = V(r)^2 r / G$ and we can find the radius of influence R_{inf} imposing:

$$M_{BH} = \frac{V(r)^2 r}{G} \quad (4.7)$$

and solving for r . Since the rotation curve $V(r)$ is not generally known with the due precision, R_{inf} does not represent a precise value but rather an order of magnitude and we can use σ_0 (velocity dispersion of the stellar component measured in the galaxy core) as an estimate of $V(r)$. Doing so we have:

$$R_{inf} = \frac{GM_{BH}}{\sigma_0} \quad (4.8)$$

4.2 Super Massive Black Holes

Is common opinion that in the core of all galaxies there is a BH of mass between 10^6 and $10^9 M_\odot$. The main observational evidences of the presence of a SMBH are the present activity in the nuclei of some galaxies, such as quasars and Seyfert galaxies and the dynamics of the material orbiting the central regions of the galaxies.

4.2.1 Measuring the SMBH mass

There are several techniques that allows to measure the mass of SMBHs. It is important to note that none of these techniques can measure the mass enclosed in a distance R_S : from this limitation comes the fact that strictly speaking we cannot speak of BH in the strict sense but rather of mass concentrations. The information we can get on SMBHs come from the following techniques:

- X-band emission
- stellar kinematics and proper motions (Milky Way and nearby galaxies)
- water masers kinematics
- ionized gas kinematics (nearby galaxies)
- reverberation mapping for active galaxies
- UV, X and nIR flare

The X emission and the UV, X and nIR flares only allow to identify the presence of a SMBH while the remaining techniques allow to measure it. All these methods differ in the distance from the SMBH we are allowed to analyze.

X-rays The X-ray emission due to BH is mainly used for the study of galactic or stellar BH and is used only marginally in the study of SMBH. In the X band there is the emission line of Fe K α emitted by fully ionized or hydrogenated iron. This line comes from extremely hot material which is located a few R_S from the center. In fact, the line profile shows a distortion due to relativistic effects of the strong gravitational field. For its nature this method is used mostly to infer the presence of a BH whose position is not known a priori.

Stellar proper motions (SMBH in the Milky Way) The SMBH present in the center of our galaxy is studied thanks to the possibility of measuring the proper motion and radial velocities of stars in the central parsecs of our galaxy. Of the main stars of the MW we know both the proper motion and the radial velocity, therefore we know the motion in the three-dimensional space. In particular there is a star, S2, that is in a bounded and strongly elliptical orbit around SgrA*, with a period of 15.2 years, a pericenter at 17 light hours and a semimajor-axis of 5.5 light days. This star alone has allowed to obtain a mass of $3.7 \cdot 10^6 M_\odot$. There are no assumptions except that on the stellar mass distribution. The measurement implies a stellar mass of $10^{17} M_\odot/\text{pc}^3$ excluding that the mass concentration may be due to a cluster of strange stars or particles and demonstrating the presence of a SMBH in the center of our Galaxy. Recently, improved measurements indicated a mass of $3.61 \cdot 10^6 M_\odot$ with an uncertainty of 10%.

It is interesting to compute the radius of influence of SgrA*, knowing that $\sigma_0 \simeq 100 \text{ km/s}$, we have $R_{infl} = 1.55 \text{ pc}$ that from our position corresponds to 40 arcsec.

In the position of the SMBH have been observed some **light flares** that were interpreted as the emission of material falling into the BH. Generally these phenomena are associated to gas accretion.

Water masers Historically water maser emission have been identified in a large number of regions of star formation. They are thought to be the result of excitation of warm interstellar gas at 1000 K.

The maser emission of NGC 4258 and that of four other AGNs is five order of magnitude brighter than the normal galactic source. Based on the dimension of the region from which the emission originates, it is not due to the superposition of multiple stellar sources: it is more likely that it is due to the active nucleus and that the emission comes from the obscuring torus present in the AGN. Using radio observations is possible to derive a rotation curve very spatially accurate. From the keplerian part of the curve is possible to derive the central mass.

Ionized gas kinematics Another trace that can be used to measure the mass of SMBH is the ionized gas. Some spheroids have gas and dust in the central regions. This type of measurement is used to study SMBHs in moderately distant galaxies such as that of the Virgo Cluster: if we calculate R_{inf} of a typical galaxy in such a cluster we find a value of $0.7''$. With spectroscopic observations is possible to resolve the sphere of influence if we have a good spatial resolution.

Even with the best angular resolution available the kinematical information within the radius of influence is limited.

Stellar kinematics An alternative and complementary method to the study of gas kinematics is the study of the kinematics of the stellar component. The main disadvantages are that for the gas the kinematics is easier to measure and that the deprojection of the observed velocity is relatively simple. The advantages are that it can be applied to all galaxies and that the distribution of the tracer is more regular. Information on the kinematics of the stellar component are obtained from the study of absorption lines and from it we can obtain the mass distribution. To determine it we need the spatial distribution of the tracer $\nu(r)$, the velocity dispersion $\sigma(r)$ and the anisotropy $\beta(r)$. The $\nu(r)$ is obtained deprojecting the surface brightness profile, $\sigma(r)$ is obtained from kinematical measurements, $\beta(r)$ is the one we need to derive from the shape of the LOSVD (we have mass-anisotropy degeneration).

Reverberation Mapping This technique is used for active galaxies (AGN) and has the advantage that can be used regardless of the distance of the object since we don't need to resolve the sphere of influence. The downside is that it needs a considerable observational effort as it requires a spectroscopical monitoring of objects over a long period of time and the measurement of the mass is not as precise as the cases already discussed.

4.3 Scaling relations for SMBH

A first step to investigate the mechanism that lead to the formation of SMBHs is the study of the relationships that links the SMBHs to the galaxy that host them.

$M_{BH} - \sigma$ relation Is an empirical relation that relates the velocity dispersion of the stellar component as measured in the spheroid to the mass of the SMBH. The velocity dispersion σ is measured by convention within a radius of $R_e/8$. The logarithmic slope of the relation is between 4 and 5. It is important to note that the σ used in this relation is measured in the center of the galaxy but in a region sufficiently larger than the radius of influence of the BH. We are therefore comparing to independent quantities. This relation wouldn't be right if we measure σ within the radius of influence: in that case we would expect a relation of the type of $M_{BH} \propto \sigma^2$ instead of $M_{BH} \propto \sigma^{4-5}$.

This fact allows us to understand that the most massive SMBHs are the most easily measurable. This relations seems to not be related to the type of galaxy.

$M_{BH} - L_T$ relation The mass of SMBHs shows a relation with the luminosity of the spheroid. This is a consequence of the previous relation since the greater σ , the larger the mass and therefore the luminosity. While in the B-band this relation is weak, in the K-band is better defined since in this band we track the stellar population that dominates the mass of the galaxy.

Should be noted that, in the case of disk galaxies, is the luminosity of the spheroid and not that of the whole galaxy to correlate with M_{BH} .

Chapter 5

Scaling relations in elliptical galaxies

5.1 Formation of elliptical galaxies

There are two opposite scenarios which are used to explain the formation of elliptical galaxies: the **monolithic dissipative collapse** and the **hierarchical clustering**. The existence of metallicity gradients in galaxies provide a clue to discriminate between these two scenarios.

In the CM a galaxy is formed by means of a rapid gravitational collapse, with a considerable dissipation of energy, from a cloud of primordial gas. During this period star formation occurs in a short period of time. If the gravitational potential of the galaxy is sufficiently high to retain the gas, this ends up concentrating in the central region of the galaxy. Therefore new generations of stars will be richer in metals than the stars in the outer region of the galaxy, generating a negative gradient in the metallicity going from the center to the outside.

According to this scenario elliptical galaxies formed at high redshift, on shorter timescales than spiral galaxies and are made of gas and not from pre-existing stars. This model explains many observations relating to the stellar populations and in particular explains the increase in metallicity as the mass increases.

The HC scenario suggests that the galaxies that we see today are formed through a sequence of mergers of smaller objects. This scenario is the natural consequence of the Λ CDM theory, so it has the advantage of having been conceived within a cosmological framework capable of predicting the large-scale structure of the universe. An important prediction made by this model is that the relation between metallicity and velocity dispersion should be canceled during aggregation process.

In elliptical galaxies there are relations that link metallicity to σ and the (B-V) color to the total mass (expressed as the total magnitude in band B).

Color- M_B relation (photometric) We know that brightest galaxies tend to be red. One mechanism capable of generating this effect is the monolithic collapse. Think of a massive gas cloud that forms stars in a short period of time: the first supernovae will produce a large amount of hot gas rich in heavy elements. The deep gravitational well in massive galaxies retains these gas which will be incorporated in the subsequent generation of stars that will be more metallic than the previous ones and therefore more red. In less massive galaxies the gas is retained in lower quantities so the stars will be metal-poor and therefore bluer.

$Mg_2-\sigma$ relation (spectroscopic) This relation is explained in the same way as the previous one, since the velocity dispersion is a measure of the mass of a galaxy and the color gives an indication on the metallicity which can be measured using Mg_2 . However should be noted that this relation, unlike the C-M, does not depend on the distance of the objects.

5.2 Kormendy relation (I_e vs R_e)

It is easy to imagine the existence of a relation between the radius of a galaxy and its total brightness: a bright galaxy will probably be large. But how can we quantify it?

We can use the Kormendy relation that says that $R_e \propto \langle I_e \rangle^{-0.83 \pm 0.08}$ where $\langle I_e \rangle$ is the average surface brightness within $1 R_e$ (less subject to measurement errors than the value of I_e intended as $I(R_e)$). If we call L_e the brightness within $1 R_e$ then we have $\langle I_e \rangle \sim L_e^{-3/2}$.

5.3 Faber-Jackson (L vs σ_0)

This relation states that brighter galaxies also have a larger velocity dispersion, more in detail we have $L_e \propto \sigma_0^4$ where σ_0 is the velocity dispersion in the center of ellipticals.

It is important to remember that the value of σ does not depend on the distance, however there are some systematic effects that can alter the measurement. These effects are related to the opening within the value of σ is measured: using larger openings means averaging σ on large areas and therefore lowering its value. If the galaxy has a strong rotation it can present widen spectral lines and therefore increase the value of σ .

5.4 The Fundamental Plane

The Faber-Jackson and the Kormendy relations specify a connection between the luminosity and a kinematic property and between the surface brightness and the effective radius, respectively. We can then say that σ_0 , $\langle I_e \rangle$ and R_e are related to each other. The distribution of elliptical galaxies in a three dimensional parameter space (R_e , $\langle I_e \rangle$, σ_0) is located close to a plane defined by:

$$R_e \propto \sigma_0^{1.4} \langle I_e \rangle^{-0.85} \quad (5.1)$$

that in the logarithmic form become:

$$\log R_e = 0.34 \langle \mu_e \rangle + 1.4 \log \sigma_0 + \text{const.} \quad (5.2)$$

where $\langle \mu_e \rangle$ is the average surface brightness within R_e measured in mag/arcsec². The Eq. 5.2 defines a plane in this three-dimensional parameter space that is known as the **fundamental plane** (FP).

How can we explain the FP? From the scalar virial theorem, valid in stationary conditions, the kinetic energy T of a galaxy and its potential energy Ω are linked by the relation:

$$2T = -\Omega \quad (5.3)$$

therefore:

$$G \frac{M}{\langle R \rangle} = \langle V^2 \rangle \quad (5.4)$$

where $\langle V^2 \rangle$ is intended as the mass-weighted mean square velocity and $\langle R \rangle$ is the gravitational radius characteristic of the structure, also weighted on the distribution of mass.

If we set r_e as an observational defined radial dimension then:

$$\langle r_e \rangle = k_R \langle R \rangle \quad (5.5)$$

where k_R contains information on the trend of the density profile within the galaxy. Similarly we consider a quantity that measures the dynamical structure of the galaxy that, for elliptical galaxies, is the central value of velocity dispersion σ_0 :

$$\sigma_0^2 = k_V \langle V^2 \rangle \quad (5.6)$$

The parameter k_V reflects the kinematic structure of the galaxy.

Replacing Eq. 5.5 and Eq. 5.6 in Eq. 5.4 we obtain:

$$M = c_2 \sigma_0^2 r_e \quad (5.7)$$

where the parameter c_2 is defined as:

$$c_2 = (G k_R k_V)^{-1} \quad (5.8)$$

We then introduce the identity:

$$L = c_1 I_e r_e^2 \quad (5.9)$$

where we have defined $I_e = L_B(r_e)/2\pi r_e^2$ called average effective surface brightness.

Once assumed for all galaxies the same brightness profile (the de Vaucouleurs radial profile), c_1 is constant for all galaxies while c_2 depends on the mass and velocity dispersion. We thus obtain the relation:

$$r_e = (c_2 c_1^{-1}) \left(\frac{M}{L} \right)^{-1} \sigma_0^2 I_e^{-1} \quad (5.10)$$

A priori the Eq. 5.10 does not define a precise geometric plane: in every point the value assumed by c_2 and M/L could have large variations from galaxy to galaxy, and the distribution of galaxies could fill all the space. On the other hand

if all the galactic structures were strictly homologous and the M/L ratio is constant with mass (and luminosity) as a consequence of homology, then a relation of this type:

$$r_e \propto \sigma_0^A I_e^B \quad (5.11)$$

with $A = 2$ and $B = -1$ would define uniquely the physical conditions of the galaxy arranged along the plane previously defined. However from the observations the values of A and B differ for more than 3σ from the predicted values. This is the so-called "tilt" of the fundamental plane and tells us that some of the hypothesis we made are not completely correct (like assuming that M/L is the same for all galaxies). From the observations is found that $A = 1.39 \pm 0.15$ and $B = -0.9 \pm 0.1$.

5.5 The k -plane

Bender et. al introduced an orthogonal coordinate system called the k system, able to describe the FP in a more significant way. The introduced variables are built with observables without introducing any hypothesis of theoretical nature. The k -space has the advantage of providing an edge-on or a nearly face-on view of the FP of the so-called dynamically hot galaxies sustained by the macroscopic pressure due to chaotic motions of the stars.

The axes of the k -space are defined as:

- $k_1 \propto \log(M/c_2)$
- $k_2 \propto \log(c_1/c_2)(M/L)I_e^3$
- $k_3 \propto \log(c_1/c_2)(M/L)$

In the projection $k_1 - k_3$ we see an edge-on view of the plane while in the projection $k_1 - k_2$ is almost seen face-on (Fig. 5.1).

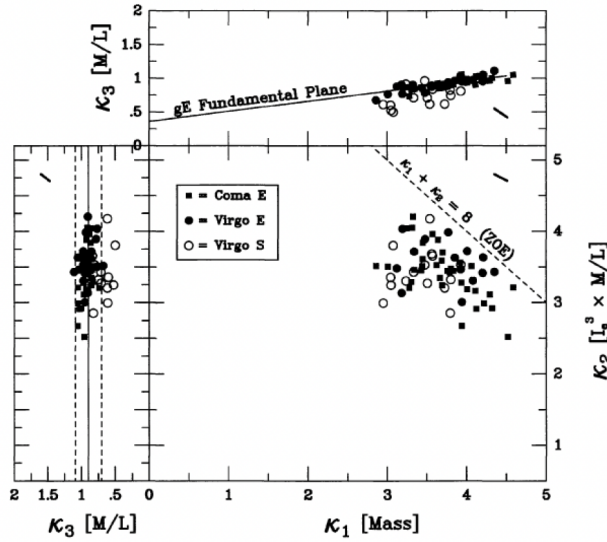


Figure 5.1: Fundamental Plane in the k -space for elliptical galaxies of Coma and Virgo, shown along the three orientations.

5.6 Evolution of the FP with z

By studying the FP at different redshift is possible to highlight a possible evolution and understand which parameter evolves the most.

Eq. 5.11, passing to logarithms can be rewritten in the form:

$$\log r_e = \alpha \log \sigma_0 + \beta I_e + \gamma \quad (5.12)$$

Variations of the slopes α and β and of the intercept γ can be interpreted as an evolution of the stellar population. If we define the dynamic mass of the galaxy as the quantity:

$$M = \frac{5\sigma_0^2 r_e}{G} \quad (5.13)$$

and assume that σ_0 and r_e do not evolve for the i -th galaxy of the cluster then:

$$\gamma^i = \log r_e^i - \alpha \log \sigma_0^i - \beta I_e^i \quad (5.14)$$

An offset from the FP ($\Delta\gamma^i = \gamma^i - \gamma \neq 0$) is linked to a difference in M/L :

$$\Delta \log \left(\frac{M}{L} \right)^i = -\frac{\Delta\gamma^i}{2.5\beta} \quad (5.15)$$

Transforming the $\Delta\gamma$ into $\Delta M/L$ and then into dynamic masses we see that the more massive systems seem to follow a passive evolution along with a high z formation epoch. Smaller systems are younger and show a greater dispersion implying a more recent star formation and/or events that rejuvenated the population.

5.7 The $D_n - \sigma$ relation

Some variables that define the FP depend on the distance (absolute magnitude, radius) while others not (σ). This means that we can use the FP to determine the distance of galaxies.

To do so we have to reduce the variables to two, one dependent on the distance and one not. It can be seen that L/Σ where $\Sigma = L/R^2$ is the surface brightness has the dimension of an area and therefore $(L/\Sigma)^{1/2}$ has the dimensions of a radio which we call D_n and represent the characteristic size of a galaxy. The actual relation is:

$$D_n \propto \sigma^{1.2} \quad (5.16)$$

where D_n is the diameter defined by a circular opening centered on the galaxy enclosing an average surface brightness of 20.75 mag/arcsec². This relation represent the FP projected along the direction in which the L/Σ plane is seen edge-on.

Using this relation is possible to derive the distance of galaxy clusters since the parameter D_n depends on the distance. In practice we have to calibrate this relation on nearby clusters whose distance is known, then we can derive the distance of the observed cluster simply looking for its position on the calibrated $D_n - \sigma$ relation.

Chapter 6

Scaling relations in spiral galaxies

6.1 Formation and evolution of spiral galaxies

According to the hierarchical clustering scenario, weak density perturbations in dark matter density distribution are sufficient to determine the evolution of primordial gas in the galaxy clusters we see today. These density fluctuations were generated during the inflation and gravitational instability has amplified them leading to the formation of dark matter halos with a certain mass spectrum.

There is a second and more empirical approach: dark matter halos were initially modeled as isothermal spheres but N-body models showed that this approach was too rough, and the profile proposed by Navarro, Frank and White which has a density cusp in the center and not a core isotherm is it more properly used to approximate the density of dark matter in the central region. The halos are composed of dark matter with a fraction of baryonic matter of approximately 5%-10%. Since collapse is a gradual process the properties of halos and galaxy disk are related.

As it cools the gas radiates energy but maintains the angular momentum, eventually settling on the disk supported by the rotation. During this process in which the gas falls towards the center, the halo responds adiabatically and contracts in the regions surrounding the disk. When a critical value is reached, **star formation** begins. The very first stars of large mass that are formed and influence the regions around them **enriching the interstellar medium with metals** that in turn influence the rate of cooling of the gas and therefore increase the collapsing speed. In addition the kinetic energy released by the supernovae will regulate the star formation by inhibiting further formation in the region around it. These metals will affect the properties of the subsequent generations of stars. The disk evolves not only by acquiring gas but also capturing dwarf galaxies from the surrounding space.

There are two techniques to model evolution of galaxies in detail: on one hand there are **complex numerical simulation** based on **N-body** simulations combined with **hydrodynamics** which allows a direct treatment of the equations without having to rely on simplistic assumptions, on the other hand we have the **semi-analytical models** which contain simplified descriptions of the various processes that act in the formation of galaxies such as the formation and evolution of dark matter halos, the cooling of the gas and its collapse.

The advantage of the second approach is that they can be used at any spatial and temporal resolution and that they are very flexible. However the latter point is also a disadvantage because the freedom in the input parameters weakens the conclusions of the results. This is the reason why the semi-analytical models need to be calibrated with observational data.

6.2 The Tully-Fisher relation

The Tully-Fisher is an empirical relation between the **magnitude** of spiral galaxies and the **gas rotation velocity** (typically HI).

The magnitude of the galaxy must be corrected for external and internal extinction since spiral galaxies can be significantly obscured by internal absorption. Obviously the magnitude must be transformed to absolute magnitude based on the distance and the gas velocity must instead be properly deprojected for the inclination.

It is possible to develop an argument similar to what was done with the FP to understand if a relation like the TF is expected or not. In the case of spiral galaxy we stars directly from the rotation velocity instead of the virial theorem like we did for the fundamental plane. Often the TF relation is used in logarithmic form.

We denote by V_0 a rotation velocity characteristic of a galaxy (maximum, flat part, fixed radius), by M the gravitating mass (baryonic and dark) and by r_c a typical radius characteristic of the galaxy, the scale radius for instance. We

then can say:

$$V_0^2 = \frac{GM}{(fr_c)} \quad (6.1)$$

where f is a factor that takes into account the structure and kinematics of the galaxy. We define some more parameters: $\alpha = M_{dark}/M_{lum}$, the ratio between the dark and luminous matter present in the galaxy, $\mu_0 = L/r_c^2$, the surface brightness characteristic of the galaxy, M_{lum}/L the mass to light ratio of the luminous component only. In this way we can write $M = (1 + \alpha)M_{lum}$ and the Eq. 6.1 can be rewritten as:

$$V_0^4 = G^2 \frac{M^2}{(f^2 R_c^2)} = L \left[\left(\frac{M_{lum}}{L} \right)^2 G^2 \frac{(1 + \alpha)^2}{f^2} \mu_0 \right] \quad (6.2)$$

M_{lum}/L depends only on the stellar population. If populations are all similar, it is constant and f is also constant if galaxies are all exponential disks, and also α . μ_0 can be seen from the observations that changes little from galaxy to galaxy. The term in square brackets contains parameters that are essentially constant in the case in which spiral galaxies are all homologous.

If all of this is true then we found an explanation of TF since Eq. 6.2 says that the total brightness L is proportional to the rotation velocity V^4 .

We can conclude that there is a regularity in the process that form disk galaxies both as regards the star formation (M_{lum}/L) and for the formation of the galaxy (α).

To determine the TF we need measurements of the galaxy's total velocity and magnitude.

Magnitude measurement Corrections are necessary for the extinction of our galaxy, knowledge of the galaxy's distance, possible K-correction. Spiral galaxies are rich in gas therefore is necessary to correct for extinction within the galaxy. The correction depends on the optical depth of the dust τ and on the fraction of light that is not obscured f . It depends on the inclination of the galaxy: the more is tilted the stronger the internal extinction as the light must pass through a thicker column of dust. Depending on the inclination i of the galaxies, extinction in magnitudes holds:

$$A^i = -2.5 \log \left\{ f(1 + e^{-\tau \sec i}) + (1 - 2f) \frac{(1 - e^{-\tau \sec i})}{(\tau \sec i)} \right\} \quad (6.3)$$

An empirical way of treating extinction considers inclination addiction as:

$$\Delta M = M_i - M_0 = \gamma \log(b/a) \quad (6.4)$$

$$\Delta M = M_i - M_0 = \gamma \log(\cos(i)) \quad (6.5)$$

where b/a is the apparent axial ratio of the galaxy and γ is a function of wavelength. In this way is possible to determine the difference in magnitude due to extinction as a function of the inclination.

However b/a is not a perfect indicator of the inclination due to a lack of galaxies with $b/a \sim 1$ (disks are not perfect circles), to a lack of galaxies with $b/a \sim 0$ (intrinsic thickness of the disk) and the fact that the bulge in galaxies that are seen edge-on, protrudes from the disk increasing the apparent thickness of the galaxy. The thing can be treated in an empirical but mathematically complex way.

Velocity measurement The rotation velocity of galaxy is measured in two way: from the **HI** (radio observations of the 21 cm line) and the **H_α** (rotation curve).

As we have already seen, typical **HI measurements** are not obtained with a very high spatial resolution but this is not a major obstacle. The zero-dimensional spectrum typically appears as a symmetric profile with two similar maxima. Assuming a priori that spiral galaxies rotate on themselves we can easily interpret the 21 cm line profile as that of a rotating disk that is not resolved spatially.

The width of the spectral line is therefore linked to the difference in velocity of the two sides of the disk: the greater the width of the line, the greater the rotation. Obviously the inclination of the disk must be taken into account.

Using the **H_α** the situation is simpler since we are able to see the velocity of the entire rotation curve.

6.3 Tully-Fisher evolution with z

The TF relation is used to determine distances similarly to the relation $D_n - \sigma$. Like the FP, the TF is used to highlight the evolution of spiral galaxies with redshift in order to find out the best scenario for the formation of the galaxies (hierarchical clustering or monolithic collapse).

6.4 Freeman Law

Freeman first described the radial surface brightness profile with the exponential law:

$$I(r) = I_0 e^{-r/h} \quad (6.6)$$

which translated into magnitudes become:

$$\mu = \mu_0 + 1.086r/h \quad (6.7)$$

Using this relation Freeman determined the central surface brightness up to $r = 0$ in galaxies where the bulge has a significant contribution. The law that describes how the central surface brightness depends on other parameters of the galaxies is:

$$\mu_B(0) = 21.7 \pm 0.3 \text{ mag arcsec}^{-2} \quad (6.8)$$

and means that μ_0 is constant for all galaxies or rather it has a Gaussian distribution of average 21.7 and sigma equal to 0.3.

6.5 Low Surface Brightness galaxies

Galaxies with $\mu_0 > 22.7$ (in band B) are defined as galaxies with low surface brightness (LSB). Today we know that LSB galaxies are known to be very numerous.

LSB galaxies seem to have followed an evolutionary history that did not lead them to position themselves in the classic Hubble sequence. LSB are generally disk-dominated and late-type or giant galaxies (Malin 1 type). They tend to have little star formation, are rich in gas and appear to be poorly developed. The HI masses are of the order of $10^9 M_\odot$ and the surface density of HI is only slightly below the critical density for starting the formation of stars. There are typically color gradients in the disk with the inner region being redder than the outer region.

We tend to interpret LSB galaxies as disk galaxies with a greater angular momentum which has counteracted their collapse. They tend to have a larger scale radius than HSB galaxies. This is the reason that has somewhat slowed down its evolution by inhibiting star formation.

LSB galaxies are very studied with regard to the distribution of dark matter as it is believed that they are also dominated in the central region.

Malin 1 Is a very peculiar galaxy that has a diameter about 6 times that of the Milky Way, an extremely low surface brightness and a huge amount of HI ($10^{11} M_\odot$) as well as a low luminosity Seyfert type core. The data seem to indicate that it is a galaxy that has not evolved and is not evolving. Its chemical composition must have changed little over time and the HI disk may have formed even at $z = 2$ to remain dormant to this day.

Chapter 7

Interstellar Medium

The space between stars is not empty at all: it contains rarefied gas, dust particles, electrons in relativistic motion, protons and other atomic nuclei. All these forms of matter are called **Interstellar medium**. One of the main differences between galaxies of different Hubble type concerns the quantity and distribution of the ISM.

7.1 ISM components

Atomic gas It is essentially **HI gas** and most of the information comes from the line radio measurements at 21 cm. It is cold gas at a temperature of 10-100 K.

There are two main observational techniques that allows to detect HI. The **single dish measurements** allows to derive, through the integrated HI flow the mass of HI and from the analysis of the line profiles the radial velocity and the amplitude of the rotational velocity.

The **aperture synthesis technique** allows us to derive detailed HI distributions and 2D velocity fields along with rotation curves. Moreover, for nearby galaxies, we can derive the cloud and inter-cloud structure of atomic ISM and temperature distributions.

HI is a very extended gas, up to 50-100 Mpc from the center, which is why is used to study the dark matter content in galaxies. Its kinematics is used to trace the gravitational potential at large radii. It rotates with a constant velocity and the single dish profile shows the typical double peak pattern from which we can measure the recession velocity and the line width. HI is about half the total baryonic mass of a typical spiral galaxy, the ratio M_{HI}/M_{tot} rises for late-type spirals. The absolute quantity of M_{HI} grows going from S0 to Sb then decreases because later types are less massive.

Molecular gas Most of the molecular gas is in form of **H₂** and partly in form of **CO** at a temperature of about 100 K. The problem is that cold gas has no observable emission lines. Most of the information is taken from rotational transitions of CO in the millimeter band with some additional information from CO isotopes or from other molecules. Data are obtained combining single-disk and aperture synthesis measurements. H₂ is found in cold and massive clouds, optically thick with mm transitions of CO. The mass of the molecular gas is empirically deduced from the correlation with the brightness of the CO.

It is important to examine the distribution of CO:

- in spirals the CO tends to follow the distribution of stars, especially the young ones;
- there is little to no CO beyond the optical radius in many low mass galaxies

The content of molecular gas increases going from late to early type galaxies becoming the dominant phase in the latter.

Interstellar dust About the 1% of the ISM is in the form of solid grains that contain about 50% of the heavy elements of the ISM. These grains absorb about 40% of the bolometric energy of galaxies in the local universe. It is possible to study the dust modeling the observed extinction in the visible and UV bands. The grains re-emit energy in the mid-IR (5-300 μm) and is possible to map the structure of the dust directly. The emission of the dust is fitted as the sum of four components:

- $T \sim 15 \text{ K}$: cold dust in molecular clouds (100-500 μm)
- $T \sim 20 - 30 \text{ K}$: dust diffuse in clouds (100-150 μm)

- $T \sim 60$ K: warm grains in star formation regions ($50 \mu\text{m}$)
- $T \sim 300$ K: PAH-band emission for small grains ($10 \mu\text{m}$)

The important feature of the IR emission is that traces the morphology of dust bands and regions of star formation.

Warm ionized ISM This ISM is at temperature of approx $10^3 - 10^4$ K. In this category there are **HII regions**, which directly trace massive star formation and are traced by hydrogen recombination lines ($\text{H}\alpha$, $\text{P}\alpha$, $\text{Br}\gamma$) or thermal radio continuum, and **diffuse ionized gas** with a characteristic density of $0.01\text{-}0.1 \text{ cm}^{-3}$ and which in spirals is primarily photoionized by UV radiation escaping HII regions, while in early type galaxies may be a diffused phase which is ionized by shocks. Sometimes is associated with diffuse neutral phase.

Hot ionized ISM (coronal) Has a temperature of about $3 - 5 \cdot 10^5$ K and is primarily traced via soft X-ray bremsstrahlung emission or high ionization UV absorption lines. The high temperatures require kinetic source for the heating energy (supernovae, stellar winds, cloud-cloud collisions). There are several structure in this category:

- diffuse halos in or around massive E/S0 galaxies or bulges
- diffuse emission from the disk due to supernova residues, stellar winds
- extra-planar fountains, super-winds
- in-falling clouds, cooling flows

7.2 Radio continuum and IR luminosity

In Fig. 7.1 we can see the close correlation between the radio continuum and the IR brightness in different types of galaxies. The fact that different galaxies show the same correlation suggests that these two parameters are generated by the same process which is the formation of massive stars. The same correlation exists between radio continuum and the cold component of the ISM and indicates a tight physical correlation between cold gas, star formation and supernovae.

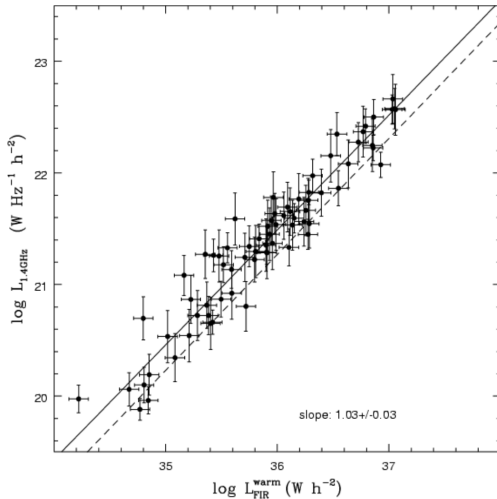


Figure 7.1: Correlation between the luminosity of the radio continuum and the IR luminosity

7.3 ISM in disk galaxies

7.3.1 Radial distribution

Fig. 7.2 shows the surface density $N(\text{H}_2)$ and $N(\text{HI})$ as a function of the radius of a Sc galaxy and the B-band surface brightness profile. H_2 is much more concentrated in the center with respect to HI . Moreover the distribution of HI has a slight depression in the center and is more extended than the distribution of the starlight. HI allows us to derive the circular velocity and the mass of the galaxy as a function of the radius.

The HI stops abruptly. The reason is that HI exists only if it is protected by totally ionized material that prevents

photons coming from the cosmic background from ionizing the HI. When the column density of this protective layer falls below a certain threshold, the HI decreases sharply.

The fraction of ISM is greater in later type than in early type spirals. In fact the average value of M_{gas}/M_{dyn} (where $M_{gas} = M_{HI} + M_{H_2}$ and M_{dyn} is the total mass of the galaxy) increases going from Sa to Sc because the amount of M_{HI} that increases with respect to M_{H_2} .

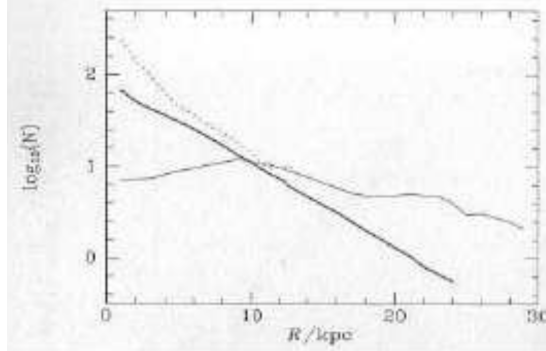


Figure 7.2: Radial distribution of the ISM in a disk galaxy. The central dark line shows the central surface brightness in the B-band, the dashed line is the density of H_2 and the dotted line is the density of HI.

7.3.2 Azimuthal distribution

Spiral structure The spiral structures are traced both by H_2 and HI as we can see in Fig. 7.3. The figure on the left shows that the emission peaks of CO are on the concave part of the spiral arms and that the gas moves from the concave side to the convex side. From the right figure is evident that where we have HI peaks the CO is in convex areas (opposite of CO peaks). This shows how both HI and H_α derive from heating and dissociation of molecular gas of short-lived hot stars.

Generally HI arms are related to the optical ones.

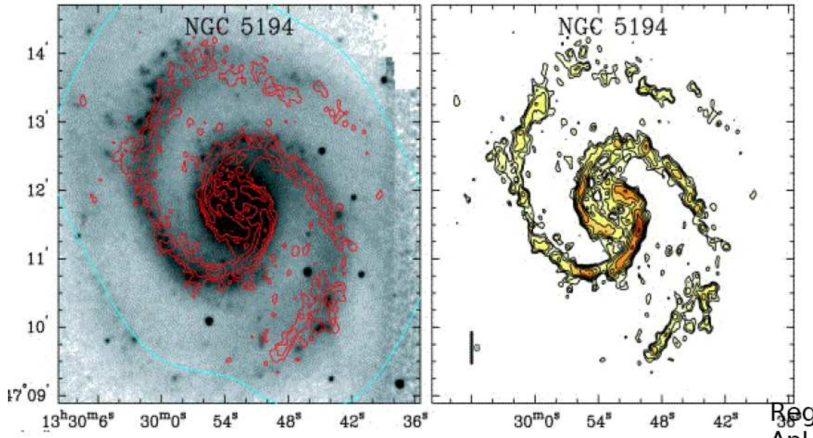


Figure 7.3: Correlation between CO and HI emissions in the spiral arms. The left panel shows the overlap of the outlines of the CO emission, the one in the right shows the same contour of the CO emission superimposed on that of HI.

Lop-sidedness In Fig. 7.4 we can see the distribution of HI and the phenomenon called lop-sidedness (asymmetry, inequality): HI appears to extend much more in one direction rather than another. From the figure we see that the isodensity lines are almost circular near the center while at large radii are not concentric with the nucleus so the large-radius gas is displaced with respect to the nucleus. This phenomenon can be seen through the velocity profile: one of the two peaks will be more pronounced.

7.3.3 Metallicity

The metallicity of the ISM of disk galaxies is estimated from the emission intensity of the spectrum in the HII regions. The idea behind this approach is that the intensity of the metal lines with respect to those of the hydrogen increase with metallicity. In practice we have to compare the $H\beta$ with the forbidden lines of O^+ , O^{2+} , N^+ and S^+ .

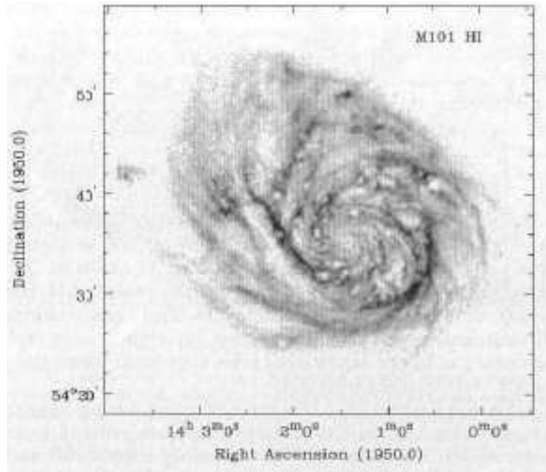


Figure 7.4: A map of M101 in the 21 cm that shows the phenomenon of lop-sidedness: the HI appears to extend more towards the northeast with respect to the opposite direction.

We know that the spectrum of the HII regions depends only on the distance from the galactic nucleus. So in spectra of HII regions located at a great distance from the center the emission lines of O^{2+} are intense while in regions closer to the center we have intense O^+ and N^+ so metallicity decreases with increasing r .

The temperature of the ISM depends on the metallicity. The spectrum is even controlled by the fraction of atoms of a given element that are in a given state of ionization.

There is also a clear correlation between the absolute magnitude of a galaxy and the metallicity that is obtained extrapolating [O/H] inside the disk: less bright galaxies tend to be poorer in metals than brightest galaxies. And since we have a correlation between the circular velocity and the luminosity of a galaxy (Tully-Fisher), we also have a correlation between the metallicity and v_c .

7.3.4 Star formation

From the H_α we can measure the number of ionizing photons (from massive young stars) that impact on the ISM. Assuming a particular distribution for spectral type we obtain the total mass of gas in these stars from the rate of photon production. If we assume that the SFR of massive stars has been constant over the relatively short lifetimes of these objects we can infer the rate at which massive stars are forming from the numbers currently present.

Hence the observations of H_α luminosity of a disk galaxy allows us to derive more or less directly the SFR of massive stars.

Outside the nucleus the H_α emission is proportional to the surface brightness function. Schmidt hypothesized that the SFR is proportional to the power of the surface density of the ISM:

$$I(H_\alpha) \propto \Sigma_{gas}^{1.3} \quad (7.1)$$

We note that a gas disk is unstable to asymmetric perturbation when Σ exceeds $\Sigma_{crit} = kv_s/\pi G$ where v_s is the speed of sound in the gas.

7.4 S0 galaxies

S0 galaxies can be considered intermediate between ellipticals and spirals. This is confirmed by the HI distribution: S0 contains more HI than ellipticals but less than spirals.

HI is concentrated in rings rather than disks and the disks of barred S0 are free of gas for a radius three times more extended than the bar. Dusts are responsible for weak lenses and are cause of the strong IR emissions. The X-emission confirm the presence of hot gas, which is typical of elliptic galaxies.

We can distinguish external disks (beyond $1.8 R_{25}$) and internal (within $0.7 R_{25}$). They often turn out to be very inclined with respect to the galactic plane and between them, in some extreme cases they are even perpendicular to the galactic plane. In the case the gas rotates in a ring above the poles of the galaxy we speak of "polar-ring galaxy". The gas that is lost by the stars of the galaxy co-rotates with the stellar component while the acquired one can also counter-rotate.

7.5 ISM in elliptical galaxies

Ellipticals contain mostly hot plasma ($T \geq 10^6$ K) that produces X-rays via bremsstrahlung, bound-free processes and emission lines. From observations it has been possible to deduce that the plasma has a distribution that is almost spherical rather than being organized in disks.

In elliptical galaxies the intensity of the optical emission is proportional to the stellar density ($j_{opt} \propto n_*$) while the X intensity is proportional to the square of the density of plasma n_e . Thus if $j_X \propto j_{opt}$ then $n_e \propto n_*^{1/2}$: the gas density falls off with radius more slowly than the stellar density in such a way that it conspires to make the brightness profile similar. This is due to the fact that plasma temperature is higher than the kinetic temperature of the stellar distribution. In fact if $n_* \propto r^{-\alpha}$ then $n_e \propto r^{-\alpha\beta}$ where $\beta = T_*/T$ is the ratio of the stellar and plasma temperature. For ellipticals $\beta \sim 0.5$.

From the X brightness and the temperature radial profile is possible to obtain the mass of the plasma ($\leq 10^{11} M_\odot$): ellipticals brighter in the X have more gas and vice versa.

7.5.1 Cold gas in elliptical galaxies

Most elliptical galaxies are poorer in cold gas than spirals of the same luminosity. This lack of cold gas makes it difficult to observe ellipticals at 21 cm or in the far IR (lack of HI, H₂ and CO). However observations show that over three quarters of bright elliptical galaxies have presence of dust in the form of cold gas and grains and the presence of emission lines as H _{α} can be detected. The origin of this cold gas is probably due to acquisition events. Another feature is that this gas is very concentrated.

Observations of dust lanes in ellipticals show that they do not contain material that has condensed on the outside of the galaxy's ISM. Observations of the cold gas emission lines show that the gas can rotate around the major axis of the galaxy while the stellar spectrum (absorption lines) show that stars tend to rotate around the minor axis of the axis. The two angular momentum vectors may turn out to be perpendicular (or inclined or anti-parallel).

One last fact concerns galaxies with active nuclei: they are much brighter in the radio due to the higher emission of cosmic rays compared to normal galaxies with equal IR brightness. Is therefore easy to understand that luminosity is correlated with IR brightness.

Chapter 8

Dark Matter

According to the cosmological scenario with cosmological constant and cold dark matter (Λ CDM) the 73% of the mass in the universe is made up of dark energy, the 23% of dark matter and only the 4% of baryonic matter. Of the baryonic matter, only the 8% is composed by luminous material, the rest (baryonic dark matter) is composed of gas or stellar remnants (primordial white dwarfs or MACHOs). Non-baryonic dark matter is composed of particles that we don't know yet.

Dark matter is necessary for three main reasons:

1. cosmological models of structure formation: these are not able to form without the help of dark matter;
2. the dynamics of galaxies and clusters of galaxies indicate the presence of dark matter;
3. from the observations of the cosmic background we know that the universe has a flat geometry and this is not possible without the presence of dark matter.

8.1 Cosmological scenario and dark matter

We know that the mass of galaxies must be much greater than the luminous/baryonic one. We can deduce the presence of some extra matter only from its gravitational effects. For example galaxies in clusters must drift apart quickly if the only attraction is the one coming from baryonic matter. Another evidence is the fact that the Local Group is moving towards a point in the sky called the Great Attractor: however, if we point a telescope in this direction, there is nothing particular so this in this point there could be a huge aggregate of dark matter.

The main open question is the nature of this dark matter: it could be made up of small objects such as brown dwarfs or the so-called MACHOs, or black holes. It could also be made up of some form of non-ordinary and non-baryonic matter.

Various experimental evidences indicate that $\Omega = 1$ (density of the universe in units of critical density) and $\Omega_{matter} \approx 0.27$: the nature of the missing matter can't only be baryonic.

Non-baryonic dark matter can be classified in two categories, hot and cold, depending on whether it was relativistic or no at the time of decoupling. If the particle decoupled while they were ultra-relativistic then we talk about **hot dark matter**: an example is given by some kind of massive neutrinos. In this framework, low-mass structures are not able to collapse due to thermal agitation of the neutrinos in every direction. In this case they would have formed large structures first and then these structures would have shattered into smaller objects as galaxies. This hierarchical scheme is called **top-down**. This scenario doesn't reproduce the distribution of galaxies at $z = 0$ and neither the galaxy formation at $z \sim 3 - 5$.

A kind of particle that decouples when it is in a non-relativistic state will have low velocity dispersion, close to zero. In this case we speak about **cold dark matter**. The family of models based on CDM are nowadays preferred by cosmologists. Unfortunately there are no obvious candidates for cold dark matter. The formation of galaxies in the CDM model precedes that of clusters. In particular star formation is guided by the formation of dark matter halos which constitute the potential well within which the gas can fall. The formation of structures proceeds in a so called **bottom-up** or **hierarchical way**: the first to form are small halos which then merge into more and more massive halos. This feature makes the CDM much more adherent to observational evidences than the hot dark matter.

In the CDM scenario therefore **WIMPS** (weakly interacting massive particles), slower and heavier, form relatively small structures inside which ordinary matter is attracted which gives birth to little star clusters or dwarf galaxies. Only latter, in a process called merging, these small structures attract each other forming galaxies and galaxy clusters.

The CDM model predicts that the halo profile of dark matter must be very steep toward the center and that galactic halos must be filled with substructures. Both of these predictions are not verified: dark matter halos that host galaxies appear to be way flatter than CDM predictions and the large amount of substructures is not reflected in the observations. This could be due to a CDM problem on sub-galactic scales.

Two variants of the CDM model have been proposed: the dark matter could be warm or could be weakly self-interacting.

8.2 Dark matter in spiral galaxies

The first evidence of DM in galaxies occurred in spiral galaxies. The light distribution in a disk is well described by the Freeman exponential law $I = I_0 \exp(-r/h)$ where I_0 is the central surface brightness and h is the scale radius. In the thin disk approximation it is possible to analytically derive the circular rotation curve generated by such a density distribution. By equating the centrifugal force to the centripetal force of gravity we obtain:

$$V_{disk}^2(r) = 4\pi G I_0 (M/L)_{disk} h y^2 [I_0(y) K_0(y) - I_1(y) K_1(y)] \quad \text{where } y = r/2h \quad (8.1)$$

I_0, I_1, K_0, K_1 are the modified Bessel functions while $(M/L)_{disk}$ indicates the mass to luminosity ratio of the stellar component. It can be seen that velocity is proportional to the surface brightness and the radius is present only as r/h so changing h will not change the shape of the velocity curve but will only scale it to a different radius.

All exponential disks therefore have a similar rotation curve with a V_{max} at about $2.4h$: for a typical value of $h = 3-4$ kpc V_{max} is at 10 kpc. Beyond this maximum value the velocity due to the exponential disk begins to decrease.

In a typical rotation curve we distinguish three regions: one in which the velocity increases with r , one in which it starts to decline and finally the so-called Keplerian region where $v \propto r^{-1/2}$. However this is not what we find in nature. In fact what we find is that the rotation curves tend to an asymptotic velocity without the Keplerian decline. In the standard scenario the responsible of this behavior is the dark matter.

If we decompose the rotation curve in its various components we have to remember that velocities add up quadratically so if we have a galaxy made of a disk and a halo then we have:

$$V_{total}^2 = V_{disk}^2(r) + V_{halo}^2(r) \quad (8.2)$$

8.2.1 Mass distribution models

What is the shape of these DM halos and their radial distribution of density? There are various opinions since this problem has not an easy solution. There are two main hypotheses: the **isothermal halo** and the **NFW halo**.

Spherical isothermal halo

A functional empirical form that generally well describes observational data is the so-called isothermal halo. The density profile is given by:

$$\rho = \frac{V_{max}^2}{4\pi G R_C^2 (1 + R^2/R_C^2)} = \frac{\rho_0}{1 + (R/R_C)^2} \quad (8.3)$$

where $V_{max} = \sqrt{4\pi G \rho_0 R_C^2}$ and R_C is the core radius. In the inner region there is constant density and in the outer one we have $\rho \propto R^2$. The isothermal halo has a flat rotation curve at large radii by construction and a rigid rotation curve in the center which is described by the formula:

$$V_{iso}^2(R) = 4\pi G \rho_0 R_C^2 \left(1 - \frac{R_C}{R} \arctan \frac{R}{R_C} \right) \quad (8.4)$$

NFW halo

Cosmological models based on Λ CDM in which galaxies are the result of the union of smaller halos predict that the density of the halo is not constant in the core but shows a central density cusp. This type of halo is named after the authors that proposed it (Navarro, Frank and White) and has a central density $\rho \propto R^{-1}$ (cusp):

$$\rho(r) = \frac{M_0}{r(a+r)} \quad (8.5)$$

with M_0 and a free parameters.

Distinguish between these two halos is not easy because they differ only in the central region where the luminous component dominates. A formula that approximate the different kinds of halo is the following:

$$\rho(r) = \frac{\rho_0}{(r/R_C)^\gamma [1 + (r/R_C)^\alpha]^{(\beta-\gamma)/\alpha}} \quad (8.6)$$

and the particular profiles are obtained changing the parameters α, β, γ .

8.2.2 Where does the halo end?

The halo of a bright spiral galaxy is expected to have a radius of the order of 400-500 kpc. In this case we talk about *virial radius*. In observational terms it is often indicated with the term of R_{200} which indicates the radius at which the density of the galaxy is 200 times higher than the critical density of the universe $\rho_{crit} = 3H^2/8\pi G$. Similarly we have V_{200} etc.

In the case of spiral galaxies there are not many methods to measure the density at a distance of 100-200 kpc.

8.3 Dark matter in elliptical galaxies

The dark matter component in elliptical galaxies is way more difficult to study due to the fact that they are poor in gas which allows to measure the rotation curve in spirals. We are therefore forced to use stellar kinematics (disadvantage: stars do not move in co-planar orbits and circular orbits like the gas).

To derive the mass of an elliptical galaxy using its stellar component we have to build a complete mass model solving the Boltzmann equations and deriving the distribution function. If we limit ourselves to measure the velocity and velocity dispersion we are limited by mass-anisotropy degeneration.

In the study of dark halos in elliptical galaxies it is found that the velocity dispersion of the stars tends to remain constant at large radii while it should decrease.

remember that the mass of the elliptical galaxies can be derived from the dispersion of velocities as:

$$GM(r) = -r\sigma_r^2 \left[\frac{d \ln v}{g \ln r} + \frac{d \ln \sigma_r^2}{d \ln r} + 2\beta \right] \quad \text{where } \beta = 1 - \frac{\sigma_\theta^2}{\sigma_r^2} \quad (8.7)$$

or using the equivalent equation:

$$\frac{-GM(r)}{r^2} = \frac{1}{\rho} \frac{d}{dr} (\rho \sigma_r^2) + \frac{2}{r} (\sigma_r^2 - \sigma_t^2) \quad (8.8)$$

where σ_r indicates the velocity dispersion in the radial direction while σ_t is the one in tangential direction. Assuming isotropy means $\sigma_r = \sigma_t$.

We can overcome the degeneracy if the shape of the LOSVD is measured, in particular the parameters h_3 and h_4 .

8.4 Dark matter in LSB galaxies

LSB galaxies are generally considered to be dominated by DM from the central regions, therefore they are the objects chosen when you want to study the distribution of DM in the central regions (for example to validate the various models of halo). In addition to studying the distribution of DM with mass models in this case you neglect the light component and derive the density directly from the data without applying any model, using:

$$M(R) = \int_0^R \rho(r) dV = 4\pi \int_0^R \rho(r) r^2 dr = V^2(R) \frac{R}{G} \quad (8.9)$$

that derived with respect to R we obtain

$$4\pi\rho(R)R^2 = \frac{1}{G} \frac{d}{dR} (V^2 R) = \frac{1}{G} \left(2VR \frac{dV}{dR} + V^2 \right) \quad (8.10)$$

and therefore

$$4\pi G\rho(R) = 2 \frac{V}{R} \frac{dV}{dR} + \left(\frac{V}{R} \right)^2 \quad (8.11)$$

Eq. 8.11 allows us to derive $\rho(R)$ from the rotation curve only, without the need to apply any mode. The critical point lies in the need to derive the velocity gradient which is not so easy due to errors on the velocity and position.

8.5 Dwarf galaxies

Dwarf galaxies are generally dominated by dark matter so they are the ideal place to study its properties. Moreover if they are the bricks that originated the galaxies, then we expect to find in them the primordial halos. The problem is that these objects are weak so we can study the closer one (and we are able to resolve them into stars).

The first step to study these objects is measuring the velocity of all the stars in the sky region occupied by the galaxy (Fig. 8.1) and eliminate all the field stars using radial velocity.

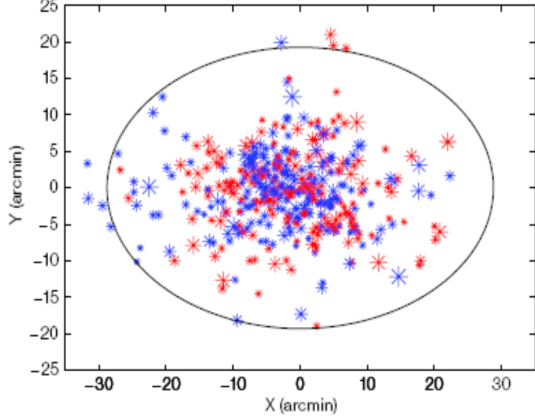


Figure 8.1: Carina dwarf galaxy. The stars that move away are shown in red, those that are approaching are colored in blue. The size of the marker is proportional to the speed module.

Once the stars have been identified they are grouped according to their distance and the velocity dispersion is calculated. The small mass of the galaxy is reflected in the small velocity dispersion value, smaller than 10 km/s which is approximately constant with the radius.

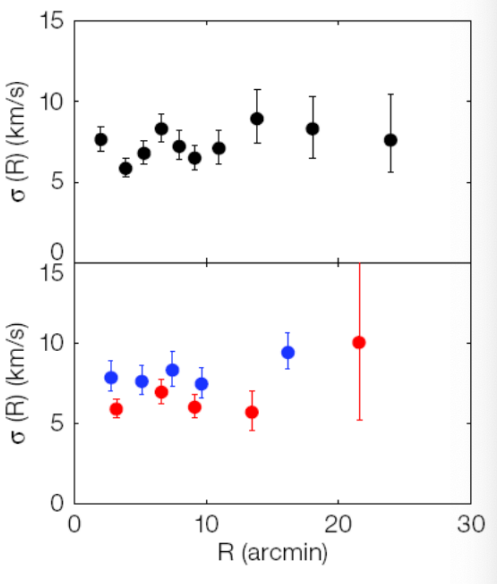


Figure 8.2: Velocity dispersion of Carina galaxy at different distances from the center. It is interesting to note that stars with higher metallicity (red) have a slightly different kinematics than stars with less metallicity (blue).

At this point kinematic data can be modeled to build a mass model: from star counts the stellar density profile is obtained. But we have a problem: how do we deal with anisotropy? We need proper motions in order to have the three dimensional velocity of all the stars. Since we don't have them we are forced to make assumptions. If we assume a spherical symmetry and an isotropic velocity dispersion we obtain a result that is not in line with an NFW halo, in the core is more similar to an isothermal halo.

8.6 Dark matter and lensing

We know that a gravitational field deflects the path of light. Measuring this deviations allows to measure the mass of the object acting as a lens. We can consider three types of lenses:

- strong lensing
- microlensing
- weak lensing

Strong lensing Is the most known lensing phenomenon. It generates images of gravitational arcs due to the fact that the light beam passing close to the mass is slowed down more than the one passing far and its wavefront is curved toward the direction of the massive source. In the case of perfect alignment the effect of the lens is to create a ring image, called **Einstein ring**, deforming the image of the source and amplifying its total brightness. The angular amplitude that the observer perceives is:

$$\theta_E = \sqrt{\frac{4GM}{c^2}} \sqrt{\frac{D_{SL}}{D_L(D_{SL} + D_L)}} \quad (8.12)$$

and depends on the mass of the lens, on the distance between the lens and the source and the one between the lens and the observer. Note that there is no dependence from the wavelength: the gravitational lens effect is perfectly **acromatic**.

Microlensing We talk of microlensing when the lens has the mass of the order of a stellar mass. An example are the MACHOS (Massive Compact Halo Objects) that are stellar compact objects with almost zero brightness that have been hypothesized to be present in the halo of the galaxy in large quantities.

When a star is exactly aligned with a MACHO the brightness of the star is amplified by the MACHO: basically the lens generates and Einstein's ring with an angular size too small to be actually observed, so we just see the increase in brightness of the source. To be sure that this increase is due to microlensing and is not an intrinsic variation it must be independent of the photometric band used.

Weak lensing In the case of weak lensing we study the small deformations that a lens causes on the background galaxies. Since these deformations are small, it is necessary to put together the information of many background galaxies to be able to actually see a signal. So we study deformations with a statistical approach to detect a preferred direction along which all galaxies are elongated. This phenomenon can be used to study the mass distribution of dark halos at virial distances from the center or to study the inhomogeneity of the diffuse dark matter in the universe. The kind of information we can get concerns the size of dark matter condensations or better information on the large-scale structure of the universe.

8.7 Alternatives to dark matter: MOND

Dark matter has been introduced because in some situations the gravity force due to visible matter is not enough. Some thought that the problem is not due to matter that we don't see but to the use of laws of gravity that are not adequate, so they proposed alternative theories according to which at a certain distance the force does not depend on the square of the distance anymore. Of the various theories the most famous is called MOND (Modified Newton Dynamics). According to MOND, when the acceleration due to gravity falls below a certain threshold, then the force does not decrease with the square of the distance but more slowly therefore it results greater at higher distance than Newton's law.

According to MOND, for gravity accelerations $a_g = F_g/m$ greater than a threshold a_0 the gravity follows the Newton's law $a = GM/r^2$ while for $a < a_0$ it changes and becomes $a = (a_0 GM/r^2)^{1/2}$. In this way rotation curves result flat and the TF is naturally generated:

$$\frac{V^4}{r^2} = a^2 = \frac{GM}{r^2} a_0 \quad (8.13)$$

from which we see $V^4 \propto M$ or $\propto L$ if M/L is constant, and that once $a < a_0$ the velocity doesn't depend on the radius. We therefore have a new universal constant a_0 .

One of the reasons for MOND is that in fact Newton's law has never been experimentally proven for such low acceleration regimes.

However his theory yields several problems: for example makes the gravitational force non-linear. An important cosmological effect concerns the relaxation time which, in the MOND regime, become much shorter.

However this is a theory that few believe but that is not discarded by the majority.